Nucleon transfer reactions below the Coulombbarrier

Nucleon Transfer Reactions Below the Coulombbarrier

by **D. Trautmann** and **K. Alder**

Institute of Theoretical Physics, Basel, Switzerland

(23. II. 70)

Abstract. A DWBA treatment for nucleon transfer reactions is given which is applicable for energies below and in the neighbourhood of the Coulomb barrier. At energies well below the Coulomb barrier the theory is essentially exact and the radial integrals describing the reaction may be evaluated analytically by means of generalized hypergeometric series. Methods for their numerical calculation are given. Semiquantal and semiclassical approximations are considered. From those it is possible to recognize a close similarity between transfer processes and Coulomb excitation. The effects of nuclear interaction, which become important at energies close to the Coulomb barrier, are treated in an approximate manner. Expressions are given for the differential and total cross-section. The deuteron stripping reaction is treated as a special case and the polarisation of the outgoing proton in (d, p)-reactions is calculated. The connection between this treatment and the diffraction model developed by Dar and Frahn and Sharaf is discussed. An improvement of the model is given. A method similar to the one used in scattering and Coulomb excitation calculations is used to improve the slow convergence of the sum over the orbital angular momenta. Comparisons with actual experiments are discussed.

1. Introduction

During the last few years there has been considerable interest in nucleon transfer reactions below the Coulomb barrier. This is due to the fact that many of the difficulties, which arise in the theoretical description of these processes at higher energies, can be avoided and consequently spectroscopic factors can be extracted with greater accuracy.

Almost all the theories used for transfer reactions are based on the distorted wave Born approximation (DWBA). In the method of Breit et al. [1–3] one calculates the probability amplitude for a neutron tunneling from the potential well of one nucleus into that of the other while the two nuclei are at rest. The relative motion of the two nuclei is described by the DWBA. This method is particularly successful at energies below the Coulomb barrier. Dar et al. [4–6] developed a diffraction model for transfer reactions. This model can be obtained from the DWBA if several simplifying assumptions are made. It can be applied particularly to reactions at high energies, where the agreement with experiment is in general quite good. A method which avoids all the approximations connected with the former models is the direct numerical calculation of the DWBA amplitude [7–8]. But, since the zero-range approximation used successfully in deuteron stripping reactions cannot be justified for general transfer reactions, this numerical calculation becomes very troublesome. The reliability

of such calculations depends furthermore quite sensitively on optical potentials used. Information on optical potentials describing the elastic scattering of heavy ions from nuclei is however rather scant. A considerable simplification results from the theory of Buttle and Goldfarb who, by extending work of Abelishvili [9], restrict themselves to energies below the Coulomb barrier [10–12]. This leads to radial integrals which can be easily evaluated.

It is the aim of this paper to show, that it is also possible to solve these radial integrals analytically, which gives a further considerable numerical simplification. It will be furthermore shown how the influence of the nuclear interaction can approximately be taken into account. This extends the validity of the theory to energies in the neighbourhood of the Coulomb barrier. In chapter 2 we summarize the well known DWBA expressions which we want to calculate for energies below and in the neighbourhood of the Coulomb barrier. This will be done in chapter 3. The radial integrals describing the reaction are quite similar to those occuring in the theory of Coulomb excitation and can be handled with the methods developed there. This will be discussed in chapter 4. In the fifth chapter it will be shown how to take into account the influence of nuclear interaction. This becomes important to energies close to the Coulomb barrier. In chapter 6 we come back to the case of pure Coulomb distortion. Using the WKB-approximation for the radial wavefunctions we obtain the so-called semiquantal and the semiclassical approximations. This results not only in a numerical simplification but also shows the great similarity between transfer reactions and the Coulomb excitation process [13]. Furthermore, since the semiclassical expressions depend only on a few general parameters, it is possible to tabulate some functions which are applicable to a large variety of reactions. The accuracy of these approximations will be estimated. Because it is interesting to test the energy dependence of the reaction we will give formulas for the total cross-section in chapter 7. In chapter 8 the special case of deuteron stripping is considered. The polarisation of the outgoing protons in (d, p)-reactions is given in chapter 9. It will be shown that polarisation measurements well below the Coulomb barrier lead to an unique determination of the angular momentum transfer j. In chapter 10 we discuss the connection between our treatment and the diffraction-models of Dar and of Frahn and Sharaf. Chapter 11 contains numerical results and a comparison between the theory and some experimental data. In performing these calculations we use a method similar to that employed in electron scattering and Coulomb excitation calculations for improving the slow convergence of the sum over the orbital angular momenta.

2. A Short Review of the DWBA-Formalism

In this chapter we summarize the basic formulas of the post-interaction form of the DWBA for one-nucleon transfer reactions. Consider a reaction of the form

$$(C + n) + T \rightarrow (T + n) + C\,, \tag{2.1}$$

where a neutron being in a state (l_1, m_1, j_1), goes from the cluster C to the target nucleus T where it will be in a state (l_2, m_2, j_2). The mass of projectile and target nucleus are denoted by a and A, respectively.

Neglecting effects of Coulomb excitation the DWBA T-matrix element can be written as

$$T_{fi} = \langle \Psi^{(-)}(\boldsymbol{r}_f)\, X_f |\, V_{nc}(\boldsymbol{r}_1)\, | \Psi^{(+)}(\boldsymbol{r}_i)\, X_i \rangle\,, \tag{2.2}$$

where $\Psi^{(-)}(\boldsymbol{r}_f)$ describes the relative motion of C in the final state and $\Psi^{(+)}(\boldsymbol{r}_i)$ gives the motion of the projectile in the center of mass system. X_f is the product of the two wavefunctions describing the internal motions of the residual nucleus $(T + n)$ and the cluster C while X_i is the corresponding product of the internal motions of projectile and target nucleus. Thus

$$\left.\begin{aligned} X_i &= \theta_{j_1 l_1} \sum_{\substack{\sigma_n \mu_1 m_1 \\ \mu_c I_c}} \langle \tfrac{1}{2}\, \sigma_n,\, l_1\, m_1 \mid j_1\, \mu_1 \rangle \langle j_1\, \mu_1,\, I_c\, \mu_c \mid I_p\, \mu_p \rangle \\ &\qquad \times \varphi_c(\xi)\, \varphi_T(\eta)\, f_{l_1 m_1}(\boldsymbol{r}_1)\, \chi^{\sigma_n}_{\frac{1}{2}}\, \chi^{\mu_c}_{I_c}\, \chi^{\mu_i}_{J_i}\,, \\ X_f &= \theta_{j_2 l_2} \sum_{\substack{\bar{\sigma}_n \mu_2 m_2 \\ \mu_i J_i}} \langle \tfrac{1}{2}\, \bar{\sigma}_n,\, l_2\, m_2 \mid j_2\, \mu_2 \rangle \langle j_2\, \mu_2,\, J_i\, \mu_i \mid J_f\, \mu_f \rangle \\ &\qquad \times \varphi_c(\xi)\, \varphi_T(\eta)\, \Phi_{l_2, m_2}(\boldsymbol{r}_2)\, \chi^{\bar{\sigma}_n}_{\frac{1}{2}}\, \chi^{\mu_i}_{J_i}\, \chi^{\mu'_c}_{I_c} \end{aligned}\right\} \tag{2.3}$$

where the X^{β}_{α}'s are spin functions and φ_i, I_i and μ_i are the internal wavefunctions, the spin and magnetic quantum numbers of particle i, respectively. The quantities $\theta_{j_1 l_1}$ and $\theta_{j_2 l_2}$ are the spectroscopic factors for the bound neutron in the initial and final state.

The coordinate system used in equation (2.2) is represented in Figure 1.

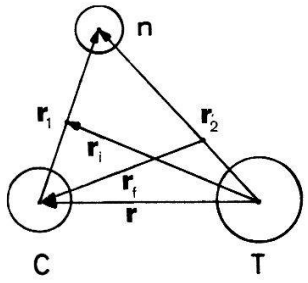

Figure 1
The system of coordinate vectors.

The vectors are mutually related as follows

$$\boldsymbol{r}_2 = \boldsymbol{r} + \boldsymbol{r}_1\,,$$

$$\boldsymbol{r}_i = \boldsymbol{r} + \frac{1}{a}\,\boldsymbol{r}_1\,, \qquad \boldsymbol{r}_f = \boldsymbol{r} - \frac{1}{A+1}\,\boldsymbol{r}_2 = \frac{A}{A+1}\,\boldsymbol{r} - \frac{1}{A+1}\,\boldsymbol{r}_1\,. \tag{2.4}$$

Assuming that the masses of C and T are large compared to the neutron mass we get:

$$\boldsymbol{r}_i \simeq \boldsymbol{r}\,, \qquad \boldsymbol{r}_f \simeq \frac{A}{A+1}\,\boldsymbol{r}\,. \tag{2.5}$$

Under these assumptions we may write for the differential cross-section:

$$\begin{aligned} \frac{d\sigma}{d\Omega} &= \frac{m_i^*\, m_f^*}{(2\pi\hbar^2)^2}\,\frac{k_f}{k_i}\,\frac{\hat{J}_f^2}{\hat{J}_i^2}\,|T_{fi}|^2 = \frac{m_i^*\, m_f^*}{(2\pi\hbar^2)^2}\,\frac{k_f}{k_i}\,\frac{\hat{J}_f^2}{\hat{J}_i^2}\,(\theta_{j_1 l_1}\,\theta_{j_2 l_2})^2 \\ &\quad \times \sum_{\alpha,\beta} \hat{\alpha}^2 \begin{Bmatrix} j_2 & \alpha & j_1 \\ l_1 & \tfrac{1}{2} & l_2 \end{Bmatrix}^2 \left| \sum_{m_1 m_2} (-)^{m_2} \begin{pmatrix} l_1 & l_2 & \alpha \\ m_1 & -m_2 & -\beta \end{pmatrix} F^{m_1, m_2}_{l_1, l_2} \right|^2 \end{aligned} \tag{2.6}$$

where we have used the notation $\hat{x} = \sqrt{2x+1}$.

The reduced masses in the entrance and exit channel are given by:

$$m_i^* = \frac{a\,A}{a+A}\,M\,, \qquad m_f^* = \frac{(a-1)\,(A+1)}{a+A}\,M \tag{2.7}$$

where M is the nucleon mass.

The transfer amplitude $F_{l_1,l_2}^{m_1,m_2}$ is defined by

$$F_{l_1,l_2}^{m_1,m_2} = \int d\boldsymbol{r}_1\,d\boldsymbol{r}\;\Psi^{(-)*}\left(\frac{A}{A+1}\,\boldsymbol{r}\right)\Phi_{l_2,m_2}^*(\boldsymbol{r}_2)\;V_{nc}(\boldsymbol{r}_1)\;f_{l_1,m_1}(\boldsymbol{r}_1)\;\Psi^{(+)}(\boldsymbol{r})\,. \tag{2.8}$$

3. The Cross Section at Low Energies

a) *With nuclear distortion*

The calculation of (2.8) may be simplified by a reasonable choice of the captured neutron wavefunction $\Phi_{l_2,m_2}^*(\boldsymbol{r}_2)$. While this wavefunction is given outside of the nucleus by a Hankel-function, we have to choose a suitable wavefunction in the nuclear interior. A form which has been shown to be quite good for low energies is the function introduced by Morinigo and El-Nadi [15–17]. So we have

$$\Phi_{l_2,m_2}^*(\boldsymbol{r}_2) = \begin{cases} N_{l_2}\,C_{l_2}\,i^{-l_2}\,r^{l_2}\,\dfrac{e^{-\varkappa r_2}}{\varkappa\,r_2}\,Y_{l_2,m_2}^*(\boldsymbol{r}_2) & \text{for} \quad r_2 < R \\ N_{l_2}\,i^{-l_2}\,h_{l_2}^{(1)}(i\,\varkappa\,r_2)\,Y_{l_2,m_2}^*(\boldsymbol{r}_2) & \text{for} \quad r_2 > R\,, \end{cases} \tag{3.1}$$

where the Hankel-function is defined by

$$h_{l_2}^{(1)}(i\,\varkappa\,r_2) = \frac{e^{-\varkappa r_2}}{\varkappa\,r_2}\sum_{k=0}^{l_2}\frac{(l_2+k)!}{k!\,(l_2-k)!}\,\frac{1}{(2\,\varkappa\,r_2)^k} \tag{3.2}$$

and $\varkappa$ is related to the binding energy of the neutron through $\varkappa = (1/\hbar)\sqrt{2\,m^*\,|E_{bin}|}$, where m^* is the reduced mass of the neutron in the exit channel. The quantity C_{l_2} is determined by the matching condition at R, namely

$$C_{l_2} = \varkappa\,R\,\frac{h_{l_2}^{(1)}(i\,\varkappa\,R)\,e^{\varkappa R}}{R^{l_2}}\,. \tag{3.3}$$

Inserting (3.1) into (2.8) we get with $\boldsymbol{r} \to -\boldsymbol{r}$:

$$\frac{d\sigma}{d\Omega} = \frac{m_i^*\,m_f^*}{(2\,\pi\,\hbar^2)^2}\,\frac{k_f}{k_i}\,\frac{\hat{J}_f^2}{\hat{J}_i^2}\,(\theta_{j_1 l_1}\,\theta_{j_2 l_2}\,N_{l_2})^2\sum_{\alpha,\beta}\hat{\alpha}^2\begin{Bmatrix} j_2 & \alpha & j_1 \\ l_1 & \frac{1}{2} & l_2 \end{Bmatrix}^2$$
$$\times\left|\sum_{m_1 m_2}(-)^{m_2+l_1}\,i^{-l_2}\begin{pmatrix} l_1 & l_2 & \alpha \\ m_1 & -\,m_2 & \beta \end{pmatrix}\left(C_{l_2}\,{}^{(1)}F_{l_1,l_2}^{m_1,m_2} + {}^{(2)}F_{l_1,l_2}^{m_1,m_2}\right)\right|^2 \tag{3.4a}$$

with

$${}^{(1)}F_{l_1,l_2}^{m_1,m_2} = \int_0^\infty d\boldsymbol{r}_1\,V_{nc}(\boldsymbol{r}_1)\,f_{l_1,m_1}(\boldsymbol{r}_1)\int_0^R d\boldsymbol{r}\;x^{l_2}\,\frac{e^{-\varkappa x}}{\varkappa\,x}\,Y_{l_2,m_2}^*(\boldsymbol{x})\;\Psi^{(-)*}(\boldsymbol{r})\;\Psi^{(+)}(\boldsymbol{r}) \tag{3.4b}$$

$${}^{(2)}F_{l_1,l_2}^{m_1,m_2} = \int_0^\infty d\boldsymbol{r}_1\,V_{nc}(\boldsymbol{r}_1)\,f_{l_1,m_1}(\boldsymbol{r}_1)\int_R^\infty d\boldsymbol{r}\;h_{l_2}^{(1)}(i\,\varkappa\,x)\;Y_{l_2,m_2}^*(\boldsymbol{x})\;\Psi^{(-)*}(\boldsymbol{r})\;\Psi^{(+)}(\boldsymbol{r}) \tag{3.4c}$$

and

$$\boldsymbol{x} = \boldsymbol{r}_1 - \boldsymbol{r}\,. \tag{3.4d}$$

For the further calculation we have to use addition theorems for the wavefunctions (3.1). We have [10, 16, 17]:

$$x^{l_2}\frac{e^{-\varkappa x}}{\varkappa x}\,Y^*_{l_2,m_2}(\boldsymbol{x}) = 4\pi\varkappa\sum_{\substack{\lambda\mu\\ LM}}(-)^{\lambda+1}\,\hat{l}_2\left(\frac{4\pi}{\hat{\lambda}}\right)^{\frac{1}{2}}\begin{pmatrix}\hat{l}_2^2\\ 2\;\lambda\end{pmatrix}^{\frac{1}{2}} r^{\lambda}\,r_1^{l_2-\lambda}$$
$$\times\begin{pmatrix}l_2-\lambda & \lambda\;\; l_2\\ -(m_2+\mu) & \mu\;\; m_2\end{pmatrix} j_L(i\varkappa r_<)\,h_L^{(1)}(i\varkappa r_>)\,Y_{l_2-\lambda}^{-(m_2+\mu)}(\boldsymbol{r}_1)$$
$$\times Y_{\lambda,\mu}(\boldsymbol{r})\,Y^*_{L,M}(\boldsymbol{r}_1)\,Y_{L,M}(\boldsymbol{r})\,, \tag{3.5a}$$

$$h_{l_2}^{(1)}(i\varkappa x)\,Y^*_{l_2,m_2}(\boldsymbol{x}) = \sqrt{4\pi}\sum_{\substack{\lambda\mu\\ LM}} i^{l_2+L-\lambda}\,\hat{L}\,\hat{l}_2\hat{\lambda}\begin{pmatrix}L\;l_2\;\lambda\\ 0\;0\;0\end{pmatrix}\begin{pmatrix}L\;\; l_2\;\; \lambda\\ M\;m_2\;\mu\end{pmatrix}$$
$$\times h_L^{(1)}(i\varkappa r_>)\,j_L^*(i\varkappa r_<)\,Y_{L,M}(\boldsymbol{r}_>)\,Y_{\lambda,\mu}(\boldsymbol{r}_<)\,, \tag{3.5b}$$

where $r_<$ and $r_>$ denotes the smaller or greater value of r or r_1, respectively.

Substituting (3.5) in (3.4), summing over the magnetic quantum numbers, integrating over the angles and using

$$\begin{pmatrix}l_1\,l_2\,\lambda\\ 0\;0\;0\end{pmatrix}\begin{Bmatrix}l_1\,l_2\,\lambda\\ j_2\,j_1\,\frac{1}{2}\end{Bmatrix} = -\frac{1}{\hat{l}_1\,\hat{l}_2}\begin{pmatrix}j_1\,j_2\,\lambda\\ \frac{1}{2}\;-\frac{1}{2}\;0\end{pmatrix}, \tag{3.6}$$

we get

$$\frac{d\sigma}{d\Omega} = 4\pi\,\frac{m_i^*\,m_f^*}{(2\pi\hbar^2)^2}\,\frac{k_f}{k_i}\,\frac{\hat{J}_f^2}{\hat{J}_i^2}\,(\theta_{j_1 l_1}\,\theta_{j_2 l_2}\,N_{l_2})^2\,.$$
$$\times\sum_{\lambda,\mu}\left|C_{l_2}\,{}^{(N)}R^{\lambda,\mu}_{l_1,l_2} + \begin{pmatrix}j_1\,j_2\,\lambda\\ \frac{1}{2}\;-\frac{1}{2}\;0\end{pmatrix}{}^{(C)}R^{\lambda,\mu}_{l_1,l_2}\right|^2, \tag{3.7a}$$

where we have used the following abbreviations:

$${}^{(N)}R^{\lambda,\mu}_{l_1,l_2} = \int_0^R d\boldsymbol{r}\,\Psi^{(-)*}\left(\frac{A}{A+1}\,\boldsymbol{r}\right)\Psi^{(+)}(\boldsymbol{r})\,Y^*_{\lambda,\mu}(\boldsymbol{r})\,r^{l_2}\,g_{l_1}(r)\,. \tag{3.7b}$$

$${}^{(C)}R^{\lambda,\mu}_{l_1,l_2} = \int_R^\infty d\boldsymbol{r}\,\Psi^{(-)*}\left(\frac{A}{A+1}\,\boldsymbol{r}\right)$$
$$\times\,\Psi^{(+)}(\boldsymbol{r})\,Y^*_{\lambda,\mu}(\boldsymbol{r})\,\{h_\lambda^{(1)}(i\varkappa r)A^{l_1}_{l_1,0}(\varkappa) - K^{l_1}_{\lambda,0}(\varkappa,r)\} \tag{3.7c}$$

with

$$g_{l_1}(r) = \sum_k a_k(L)\,r^{-k}\{h_L^{(1)}(i\varkappa r)\,A^{l_1}_{L,k}(\varkappa) - K^{l_1}_{L,k}(\varkappa,r)\}\,, \tag{3.7d}$$

$$a_k(L) = (-)^{k+L+1}\begin{Bmatrix}j_2\,\lambda\,j_1\\ l_1\,\frac{1}{2}\,l_2\end{Bmatrix}\begin{Bmatrix}l_2-k\;L\;\lambda\\ l_1\qquad l_2\;k\end{Bmatrix}\begin{pmatrix}2\,l_2\\ 2\,(l_2-k)\end{pmatrix}^{\frac{1}{2}}$$
$$\hat{L}^2\,\hat{l}_2^2\,\hat{l}_1^2\begin{pmatrix}l_2-k\;L\;\lambda\\ 0\qquad 0\;0\end{pmatrix}\begin{pmatrix}l_1\,k\,L\\ 0\,0\,0\end{pmatrix}, \tag{3.7e}$$

$$A^l_{L,k}(\varkappa) = \int_0^\infty dr\,\varphi_l^k(r)\,j_L^*(i\varkappa r)\,,\qquad \varphi_l^k(r) = r^{k+2}\,V_{nc}(r)\,f_l(r)\,, \tag{3.7f}$$

$$K^{l}_{L,k}(\varkappa, r) = \frac{1}{2}\left\{h^{(1)}_L(i\varkappa r)\int_r^\infty dr\,\varphi^k_l(r)\,h^{(2)}_L(i\varkappa r) - h^{(2)}_L(i\varkappa r)\int_r^\infty dr\,\varphi^k_l(r)\,h^{(1)}_L(i\varkappa r)\right\}. \tag{3.7g}$$

The summations contained in (3.7) are restricted by the following selection rules:

$$\begin{aligned}
&|l_2 - k - \lambda| \leqslant L \leqslant l_2 - k + \lambda\,, \quad |l_1 - l_2| \leqslant \lambda \leqslant l_1 + l_2\,,\\
&|l_1 - k| \leqslant L \leqslant l_1 + k\,, \quad |j_1 - j_2| \leqslant \lambda \leqslant j_1 + j_2\,, \quad |l_2 - k| \leqslant L \leqslant l_2 + k\,,\\
&l_1 + k + L = \text{even}\,, \qquad l_2 + L + \lambda - k = \text{even}\,.
\end{aligned} \tag{3.8}$$

While the integral ${}^{(N)}R^{\lambda,\mu}_{l_1,l_2}$ contains the whole nuclear interaction, ${}^{(C)}R^{\lambda,\mu}_{l_1,l_2}$ is determined by the Coulomb interactions only. The quantity $K^{l}_{L,k}(\varkappa, r)$ is due to penetration effects and is negligible at low energies, while the formfactor $A^{l}_{L,k}(\varkappa)$ is determined by the finite-range interaction between the neutron and the cluster C.

The integrals (3.7b) and (3.7c) can be calculated explicitely in this form only for the special case $\lambda = 0$ [10, 18]. For the general case it is necessary to introduce the partial wave decomposition for $\Psi^{(-)*}(\boldsymbol{r})$ and $\Psi^{(+)}(\boldsymbol{r})$. Thus

$$\begin{aligned}
\Psi^{(+)}(\boldsymbol{r}) &= \frac{4\pi}{k_i r}\sum_{l_i m_i} i^{l_i}\, e^{i\sigma_{l_i}(\eta_i)}\,\chi_{l_i}(k_i, r)\; Y^*_{l_i,m_i}(\boldsymbol{k}_i)\; Y_{l_i,m_i}(\boldsymbol{r})\,,\\
\Psi^{(-)*}\left(\frac{A}{A+1}\,\boldsymbol{r}\right) &= \frac{4\pi}{\bar{k}_f r}\sum_{l_f,m_f} i^{-l_f}\, e^{i\sigma_{l_f}(\eta_f)}\,\chi_{l_f}\left(k_f, \frac{A}{A+1}\,\boldsymbol{r}\right) Y^*_{l_f,m_f}(\boldsymbol{k}_f)\; Y_{l_f,m_f}(\boldsymbol{r})\,,
\end{aligned} \tag{3.9}$$

where

$$\sigma_l(\eta) = \arg\Gamma(l + 1 + i\,\eta) \tag{3.10}$$

is the usual Coulomb phaseshift and η_i and η_f are defined by

$$\eta_i = \frac{Z_C\, Z_T\, e^2\, m_i^*}{\hbar^2\, k_i}\,, \qquad \eta_f = \frac{Z_C\, Z_T\, e^2\, m_f^*}{\hbar^2\, k_f}\,. \tag{3.11}$$

Next we choose the so-called 'incident-beam-coordinate system', in which the z-axis is defined by the direction of $\boldsymbol{k}_i$ and the y-axis by $\boldsymbol{k}_i \times \boldsymbol{k}_f$.

After integrating over the angles one obtains

$$\begin{aligned}
\frac{d\sigma}{d\Omega} &= 16\pi\,\frac{a\,(a-1)\,A\,(A+1)}{(a+A)^2}\left(\frac{M}{\hbar^2}\right)^2\frac{\hat{J}_f^2}{\hat{J}_i^2}\,\frac{k_f}{k_i}\,(\theta_{j_1 l_1}\,\theta_{j_2 l_2}\,N_{l_2})^2\sum_{\lambda,\mu}\hat{\lambda}^2\\
&\times\left|\sum_{l_i,l_f} i^{l_i - l_f}\,\hat{l}_i^2\,\hat{l}_f\, e^{i(\sigma_{l_i}(\eta_i)+\sigma_{l_f}(\eta_f))}\; Y_{l_f,\mu}(\vartheta, 0)\begin{pmatrix} l_i & l_f & \lambda\\ 0 & 0 & 0\end{pmatrix}\begin{pmatrix} l_i & l_f & \lambda\\ 0 & \mu & -\mu\end{pmatrix} Q^{l_1,l_2}_{l_i,l_f}(j_1, j_2, \lambda, \varkappa)\right|^2,
\end{aligned} \tag{3.12a}$$

with

$$\begin{aligned}
Q^{l_1,l_2}_{l_i,l_f}(j_1, j_2, \lambda, \varkappa) &= C_{l_2}\,\frac{1}{k_i\,\bar{k}_f}\int_0^R dr^{(N)}\,\chi_{l_i}(r)^{(N)}\,\chi_{l_f}\left(\frac{A}{A+1}\,r\right) r^{l_2}\,g_{l_1}(r)\\
&+\begin{pmatrix} j_1 & j_2 & \lambda\\ \frac{1}{2} & -\frac{1}{2} & 0\end{pmatrix}\frac{1}{k_i\,\bar{k}_f}\int_R^\infty dr^{(C)}\,\chi_{l_i}(r)^{(C)}\,\chi_{l_f}\left(\frac{A}{A+1}\,r\right)\{h^{(1)}_\lambda(i\varkappa r)\,A^{l_1,0}_{l_1,0}(\varkappa) - K^{l_1,0}_{\lambda,0}(\varkappa, r)\}
\end{aligned} \tag{3.12b}$$

and

$$\bar{k}_f = \frac{A}{A+1} k_f \tag{3.12c}$$

ϑ is the scattering angle in the center-of-mass-system, and ${}^{(N)}\chi_l$, ${}^{(C)}\chi_l$ are the radial wavefunctions inside and outside the nucleus.

b) *Pure coulomb distortion*

For energies, which are well below the Coulomb barrier, the expression (3.12) simplifies considerably. Since the classical turning point of the projectile is in this case at a large distance from the target nucleus, the integral containing the wavefunctions ${}^{(N)}\chi_l(r)$ can be neglected. Furthermore it is quite legitimate to change the lower integration limit in the other integral to zero. The radial wavefunctions ${}^{(C)}\chi_l$ are now given by regular Coulomb wavefunctions

$$\begin{aligned} {}^{(C)}\chi_l(r) = F_l(k\,r) = e^{-(\pi/2)\eta} \frac{|\Gamma(l+1+i\,\eta)|}{2\,(2\,l+1)!} \\ \times (2\,k\,r)^{l+1} e^{-ikr}\, {}_1F_1\,(l+1-i\,\eta;\, 2\,l+2;\, 2\,i\,k\,r)\,. \end{aligned} \tag{3.13}$$

Hence we get from (3.12):

$$\frac{d\sigma}{d\Omega} = \bar{\chi}^2 \sum_{\lambda} \begin{pmatrix} j_1\, j_2\, \lambda \\ \frac{1}{2}\, -\frac{1}{2}\, 0 \end{pmatrix}^2 G_\lambda(\vartheta, \eta_i, \eta_f, \varkappa)\,, \tag{3.14a}$$

where we have used the following definitions:

$$\bar{\chi}^2 = 16\,\pi \frac{a\,(a-1)\,A\,(A+1)}{(a+A)^2} \frac{k_f}{k_i} \frac{\hat{J}_f^2}{\hat{J}_i^2} (\theta_{j_1 l_1}\, \theta_{j_2 l_2}\, N_{l_2})^2 \left| \frac{M}{\hbar^2}\, A^{l_1}_{l_1,0}(\varkappa) \right|^2, \tag{3.14b}$$

$$G_\lambda(\vartheta, \eta_i, \eta_f, \varkappa) = \sum_{\mu} |F_{\lambda,\mu}(\vartheta, \eta_i, \eta_f, \varkappa)|^2\,, \tag{3.14c}$$

with

$$\begin{aligned} F_{\lambda,\mu}(\vartheta, \eta_i, \eta_f, \varkappa) = \hat{\lambda} \sum_{l_i, l_f} i^{l_i - l_f}\, \hat{l}_i^2\, \hat{l}_f\, e^{i(\sigma_{l_i}(\eta_i) + \sigma_{l_f}(\eta_f))}\, Y_{l_f,\mu}(\vartheta, 0) \\ \times \begin{pmatrix} l_i\, l_f\, \lambda \\ 0\,0\,0 \end{pmatrix} \begin{pmatrix} l_i\, l_f & \lambda \\ 0\, \mu & -\mu \end{pmatrix} T^{\lambda,\varkappa}_{l_i, l_f} \end{aligned} \tag{3.14d}$$

and

$$T^{\lambda,\varkappa}_{l_i, l_f} = \frac{1}{k_i\, \bar{k}_f} \int_0^\infty F_{l_i}(k_i\, r)\; h^{(1)}_\lambda(i\,\varkappa\, r)\; F_{l_f}(\bar{k}_f\, r)\, dr \tag{3.14e}$$

The quantity $\bar{\chi}^2$ determines the strength of the reaction, while its angular dependence is given by $G_\lambda(\vartheta, \eta_i, \eta_f, \varkappa)$.

4. Calculation of the Coulomb Integrals

In this chapter we want to give explicit analytic expressions for the radial integrals given in (3.14). We define:

$$T^{\lambda,\varkappa}_{l_i,l_f} = \frac{1}{k_i\,\bar{k}_f}\int_0^\infty F_{l_i}(k_i\,r)\,h^{(1)}_\lambda(i\,\varkappa\,r)\,F_{l_f}(\bar{k}_f\,r)\,dr$$

$$= \sum_{n=0}^{\lambda}\frac{(\lambda+n)!}{\varkappa\,(\lambda-n)!\,n!\,(2\,\varkappa)^n}\,M^{-n-1,\varkappa}_{l_i,l_f} \tag{4.1a}$$

with

$$M^{-n-1,\varkappa}_{l_i,l_f} = \frac{1}{k_i\,\bar{k}_f}\int_0^\infty F_{l_i}(k_i\,r)\,\frac{e^{-\varkappa r}}{r^{n+1}}\,F_{l_f}(\bar{k}_f\,r)\,dr\,. \tag{4.1b}$$

This integral is quite similar to the radial integrals occuring in the theory of Coulomb excitation [13, 19, 20] and can therefore be handled with the methods developed there. Throughout this section we make use of the formulas given in the appendix of [20].

Using an integral representation for the ${}_1F_1$-function in (3.13) and changing the order of integration we obtain a function, which is identical with the integral representation of one of the so-called Appell-functions [20, IIE. 93]. This function F_2 is a generalized hypergeometric function in two variables [21–22], and is defined in the neighbourhood of $x = y = 0$ by a series expansion.

For (4.1b) we get [23, 24]:

$$T^{\lambda,\varkappa}_{l_i,l_f} = \sum_{n=0}^{\lambda}\frac{(\lambda+n)!}{n!\,(\lambda-n)!\,(2\,\varkappa)^n\,\varkappa}\,(l_i+l_f+1-n)!\,\frac{|\Gamma(l_i+1+i\,\eta_i)|}{(2\,l_i+1)!}$$

$$\times\,\frac{|\Gamma(l_f+1+i\,\eta_f)|}{(2\,l_f+1)!}\,e^{-\pi/2(\eta_i+\eta_f)}\,(k_i-\bar{k}_f+i\,\varkappa)^{n-2}\,(x)^{l_i}\,(-y)^{l_f}\,i^{(l_i+l_f-n+2)}$$

$$\times\,F_2(l_i+l_f-n+2\,,\;l_i+1+i\,\eta_i,\,l_f+1-i\,\eta_f;\,2\,l_i+2,\,2\,l_f+2;\,x,\,y)\,, \tag{4.2a}$$

with

$$x = \frac{2\,k_i}{k_i-\bar{k}_f+i\,\varkappa}\,,\qquad y = \frac{-2\,\bar{k}_f}{k_i-\bar{k}_f+i\,\varkappa}\,. \tag{4.2b}$$

The function F_2 converges only, if

$$|x|+|y|<1\,. \tag{4.3}$$

Since this is not the case, analytic continuations of the F_2-functions must be used. Such continuations lead to Appell-functions of the argument $1/x$ and $1/y$. Two especially simple analytic continuations can be found immediately. If $n=0$ and $l_i = l_f = l$, we get [20, IIE. 96]:

$$M^{-1,\varkappa}_{l,l} = \frac{|\Gamma(l+1+i\,\eta_f)|\,|\Gamma(l+1+i\,\eta_i)|}{(2\,l+1)!}\,(-x_0)^l\left(\frac{k_i-\bar{k}_f-i\,\varkappa}{k_i+\bar{k}_f-i\,\varkappa}\right)^{i\eta_f}$$

$$\times\left(\frac{k_i-\bar{k}_f+i\,\varkappa}{k_i+\bar{k}_f-i\,\varkappa}\right)^{i\eta_i}\frac{e^{-[(\pi/2)\xi]}}{(k_i-\bar{k}_f)^2+\varkappa^2}$$

$$\times\,{}_2F_1(l+1-i\,\eta_i,\,l+1-i\,\eta_f;\,2\,l+2;\,x_0) \tag{4.4a}$$

with

$$\xi = \eta_f - \eta_i\,, \qquad x_0 = -\frac{4\,k_i\,\bar{k}_f}{(k_i-\bar{k}_f)^2+\varkappa^2}\,. \tag{4.4b}$$

For the so-called 'maximal matrixelements' (the name comes from the theory of Coulomb excitation), with $l_i = l_f \pm n$, we get [20, IIE. 98, 99]

$$\begin{aligned} M^{-n-1,\varkappa}_{l+n,l} &= e^{-[(\pi/2)\xi]}\left|\frac{\Gamma(l+1+i\,\eta_f)}{\Gamma(l+n+1+i\,\eta_i)}\right|\left(\frac{\bar{k}_f}{k_i}\right)^l (2\,k_i)^{n-2} \\ &\times\left\{\frac{|\Gamma(n+i\,\xi)|}{(2\,n-1)!}\,F_2\left(-2\,n+1,\, l+1-i\,\eta_f,\, l+1+i\,\eta_f,\right.\right. \\ &-n+1-i\,\xi,\,-n+1+i\,\xi;\,\frac{k_i-\bar{k}_f-i\,\varkappa}{2\,k_i},\,\frac{k_i-\bar{k}_f+i\,\varkappa}{2\,k_i}\Bigg) \\ &+2\,Re\left[\left(e^{i\pi}\,\frac{k_i-\bar{k}_f-i\,\varkappa}{2\,k_i}\right)^{n+i\xi}\frac{\Gamma(l+n+1-i\,\eta_i)\,\Gamma(-n-i\,\xi)}{\Gamma(l+1-i\,\eta_f)}\right. \\ &\times F_2\left(-n+1+i\,\xi,\, l+n+1-i\,\eta_i,\, l+1+i\,\eta_f;\right. \\ &\left.\left.\left.n+1+i\,\xi,\,-n+1+i\,\xi;\,\frac{k_i-\bar{k}_f-i\,\varkappa}{2\,k_i},\,\frac{k_i-\bar{k}_f+i\,\varkappa}{2\,k_i}\right)\right]\right\}. \end{aligned} \tag{4.5}$$

If $n=0$, equation (4.5) reduces to (4.4). The first F_2-function in (4.5) is a polynomial, since the first parameter is a negative integer. Especially for $n=1$ we get:

$$\begin{aligned} &F_2\left(-1,\, l+1-i\,\eta_f,\, l+1+i\,\eta_f;\,-i\,\xi,\,+i\,\xi;\right. \\ &\left.\frac{k_i-\bar{k}_f-i\,\varkappa}{2\,k_i},\,\frac{k_i-\bar{k}_f+i\,\varkappa}{2\,k_i}\right) = \frac{\eta_f\,\bar{k}_f-\eta_i\,k_i-(l+1)\,\varkappa}{k_i\,\xi} \end{aligned} \tag{4.6}$$

Also in this case, the second F_2-function in (4.5) can be transformed into a F_1-function [20, IIE. 97], which converges more rapidly than the original function F_2, i.e.:

$$\begin{aligned} &F_2\left(i\,\xi,\, l+2-i\,\eta_i,\, l+1+i\,\eta_f;\, 2+i\,\xi,\, i\,\xi;\,\frac{k_i-\bar{k}_f-i\,\varkappa}{2\,k_i},\,\frac{k_i-\bar{k}_f+i\,\varkappa}{2\,k_i}\right) \\ &= \frac{(k_i+\bar{k}_f+i\,\varkappa)^{1+2i\eta_i}}{(2\,\bar{k}_f)^{2l+1}}\left(\frac{2\,k_i}{k_i+\bar{k}_f-i\,\varkappa}\right)^{i\xi} \\ &\times\left((k_i+\bar{k}_f)^2+\varkappa^2\right)^{l-i\eta_i} F_1\left(-l+i\,\eta_f,\,-(l+1+i\,\eta_i),\,2,\,2+i\,\xi;\right. \\ &\left.\frac{(k_i-\bar{k}_f)^2+\varkappa^2}{(k_i+\bar{k}_f)^2+\varkappa^2},\,\frac{k_i-\bar{k}_f-i\,\varkappa}{k_i+\bar{k}_f+i\,\varkappa}\right). \end{aligned} \tag{4.7}$$

For the calculation of the other maximal matrixelements we use the symmetry relation

$$M^{-n-1,\varkappa}_{l_i,l_f}(\eta_i,\eta_f) = M^{-n-1,\varkappa}_{l_f,l_i}(\eta_f,\eta_i)\,. \tag{4.8}$$

If $l_i \neq l_f \pm n$, we do not get simple analytic continuations of the F_2-function. It is possible to obtain an explicit expression by using equation (IIE. 103) of [20], but the result is lengthy and the numerical calculation of it is rather tedious. Other possibilities for an analytic continuation are the relations derived by Olsson and Hahne [25–27]. We prefer, however, to calculate the general matrixelement by means of recursion relations. The existence of such recursion formulas is a consequence of the simple recursion properties of contiguous hypergeometric functions and of the Coulomb wavefunction. The use of the two well known recursion relations for the Coulomb wavefunction

$$(l+1)\frac{dF_l(k\,r)}{k\,dr} = \left(\frac{(l+1)^2}{k\,r} + \eta\right) F_l(k\,r) - |l+1+i\,\eta|\,F_{l+1}(k\,r)$$

$$l\frac{dF_l(k\,r)}{k\,dr} = |l+i\,\eta|\,F_{l-1}(k\,r) - \left(\frac{l^2}{k\,r} + \eta\right) F_l(k\,r) \tag{4.9}$$

leads immediately to the following result:

$$x_1\,C^f_{l_f,1}\,q\,M^{-n-1,\varkappa}_{l_i,l_f+1} + x_2\,C^i_{l_i,0}\,M^{-n-1,\varkappa}_{l_i-1,l_f} - x_3\,C^i_{l_i,1}\,M^{-n-1,\varkappa}_{l_i+1,l_f} - x_4\,C^f_{l_f,0}\,q\,M^{-n-1,\varkappa}_{l_i,l_f-1}$$
$$-\left(x_1\left(\frac{1}{l_f+1} - \bar{\varkappa}\right)q + x_2\frac{1}{l_i} - x_3\frac{1}{l_i+1} - x_4\left(\frac{1}{l_f} + \bar{\varkappa}\right)q\right) M^{-n-1,\varkappa}_{l_i,l_f}$$
$$= \frac{1}{k_i\,\eta_i}\left(x_1\,(l_f-n) + x_2\,l_i - x_3\,(l_i+1) - x_4\,(l_f+n+1)\right) M^{-n-2,\varkappa}_{l_i,l_f} \tag{4.10a}$$

where we have used the definitions:

$$q = \frac{\bar{k}_f\,\eta_f}{k_i\,\eta_i}, \qquad \bar{\varkappa} = \frac{\varkappa}{\bar{k}_f\,\eta_f}, \qquad C^x_{l,p} = \frac{|l+p+i\,\eta_x|}{\eta_x\,(l+p)} \tag{4.10b}$$

and where the x_i are arbitrary constants, satisfying the condition

$$x_1 + x_2 + x_3 + x_4 = 0\,. \tag{4.11}$$

Giving these factors appropriate values we obtain the wanted recursion relations. Starting with the maximal matrixelements $M^{-1,\varkappa}_{l,l}$ and $M^{-2,\varkappa}_{l+1,l}$ we obtain

$$M^{-1,\varkappa}_{l+1,l} = \frac{1}{\dfrac{\bar{k}_f\,\eta_f - k_i\,\eta_i}{l+1} - \varkappa}\left\{k_i\,\eta_i\,(C^f_{l,1}\,q\,M^{-1,\varkappa}_{l+1,l+1} - C^i_{l,1}\,M^{-1,\varkappa}_{l,l}) + M^{-2,\varkappa}_{l+2,l}\right\}. \tag{4.12}$$

All matrixelements necessary for the calculation of (4.1) (with l_i, l_f and λ arbitrary) can now be obtained by repeated application of the recursion relations (see section 11.a)

$$M^{-n-1,\varkappa}_{l+p+1,l} = -\frac{C^f_{l,1}}{C^i_{l,p+1}}\,q\,\frac{(2\,l+2\,p+1)}{(p+n)}\,M^{-n-1,\varkappa}_{l+p,l+1} +$$
$$+\frac{C^i_{l,p}}{C^i_{l,p+1}}\,\frac{(2\,l+p+1-n)}{(p+n)}\,M^{-n-1,\varkappa}_{l+p-1,l} - \frac{(2\,l+2\,p+1)}{C^i_{l,p+1}\,(p+n)}$$
$$\times\left(\frac{l+1-n}{(l+p)\,(l+p+1)} + q\left(\bar{\varkappa} - \frac{1}{l+1}\right)\right) M^{-n-1,\varkappa}_{l+p,l} \tag{4.13a}$$

$$M_{l+p,l}^{-n-2,\varkappa} = \frac{k_i\,\eta_i}{2\,l+1+p-n}\left\{C_{l,1}^{f}\,q\,M_{l+p,l+1}^{-n-1,\varkappa} + C_{l,p+1}^{i}\,M_{l+p+1,l}^{-n-1,\varkappa}\right.$$
$$\left. - \left(q\left(\frac{1}{l+1}-\bar{\varkappa}\right)+\frac{1}{l+p+1}\right)M_{l+p,l}^{-n-1,\varkappa}\right\} \tag{4.13b}$$

and with the symmetry relation (4.8).

A further simplification of the numerical procedure can be obtained by using recursion relations for the maximal matrixelements.

Using the fact that three contiguous ${}_2F_1$-functions are always linearly dependent, we get with (4.4)

$$z_1\,M_{l+1,l+1}^{-1,\varkappa} + z_2\,M_{l,l}^{-1,\varkappa} + z_3\,M_{l-1,l-1}^{-1,\varkappa} = 0 \tag{4.14a}$$

with

$$z_1 = l\,|l+1+i\,\eta_i|\,|l+1+i\,\eta_f|\,,$$
$$z_2 = -(2\,l+1)\left\{l\,(l+1)\left(1-\frac{2}{x_0}\right)+\eta_i\,\eta_f\right\}\,,$$
$$z_3 = (l+1)\,|l+i\,\eta_i|\,|l+i\,\eta_f|\,, \tag{4.14b}$$

and where x_0 is given by (4.4b).

An analogous relation exists between four F_1-functions, i.e.

$$F_1\,(\alpha+n_1,\beta+n_2,\beta'+n_3,\gamma+n_4;x,y)$$
$$= \left((A(x,y)+B(x,y)\,\frac{\partial}{\partial x}+C(x,y)\,\frac{\partial}{\partial y}\right)F_1(\alpha,\beta,\beta',\gamma;x,y) \tag{4.15}$$

where the n_r are arbitrary negative or positive integers and A, B and C are rational functions in x and y [18]. For example

$$F_1(\alpha+1,\beta+1,\beta'+1,\gamma+2;x,y)$$
$$= \frac{\gamma\,(\gamma+1)}{\alpha\,(\gamma-\alpha)}\left\{\frac{1}{\beta}\,\frac{x-1}{x-y}\,\frac{\partial}{\partial x}+\frac{1}{\beta'}\,\frac{y-1}{y-x}\,\frac{\partial}{\partial y}\right\}F_1(\alpha,\beta,\beta',\gamma;x,y)\,. \tag{4.16}$$

Following [22] one obtains

$$\frac{A_1\,C_{02}-A_2\,C_{01}}{R\,(l-1)}\,M_{l+\lambda-1,l-1}^{-\lambda-1,\varkappa}+\frac{B_1\,C_{02}-B_2\,C_{01}}{R(l)}\,M_{l+\lambda,l}^{-\lambda-1\varkappa}$$
$$-\frac{B_0\,C_{02}}{R\,(l+1)}\,M_{l+\lambda+1,l+1}^{-\lambda-1,\varkappa}+\frac{B_0\,C_{01}}{R\,(l+2)}\,M_{l+\lambda+2,l+2}^{-\lambda-1,\varkappa}=0\,, \tag{4.17a}$$

where the following abbreviations were used:

$$R\,(l+n) = \frac{|\Gamma\,(\alpha+n+1)|\,|\Gamma\,(\beta+n+1)|}{(\gamma+2\,n+1)!}\,(-x\,y)^{l+n}\left(\frac{\bar{k}_f}{k_i}\right)^{l+n}\,, \tag{4.17b}$$

$$\alpha=\lambda+l+i\,\eta_i\,,\quad \beta=l+i\,\eta_f\,,\quad \beta'=l-i\,\eta_f\,,\quad \gamma=2\,l+2\,\lambda\,, \tag{4.17c}$$

$$x = \frac{2k_i}{k_i - \bar{k}_f + i\varkappa}, \qquad y = \frac{2k_i}{k_i + \bar{k}_f + i\varkappa}, \tag{4.17d}$$

$$S_0^x = \frac{\beta'}{x-y}, \qquad S_1^x = \frac{\alpha\beta}{x(1-x)},$$

$$S_2^x = -\frac{1}{x}\left(\frac{\beta' y}{x-y} + \frac{\gamma - x(\alpha+\beta+1)}{1-x}\right), \quad S_3^x = \frac{\beta y}{x}\frac{1-y}{(x-y)(1-x)}, \tag{4.17e}$$

$$S_i^y(x, y; \beta, \beta') = S_i^x(y, x; \beta', \beta), \tag{4.17f}$$

$$M_n = \frac{(\gamma+2n)(\gamma+2n+1)}{(\gamma-\alpha-n)(\alpha+n)(\beta+n)}\frac{x-1}{x-y},$$

$$N_n(x, y; \beta, \beta') = M_n(y, x; \beta', \beta), \tag{4.17g}$$

$$B_0 = M_0, \qquad C_i(x, y; \beta, \beta') = B_i(y, x; \beta', \beta), \tag{4.17h}$$

$$A_1 = M_1 M_0 S_1^x + N_1 N_0 S_1^y, \tag{4.17i}$$

$$B_1 = N_1\frac{\partial M_0}{\partial y} + M_1\frac{\partial M_0}{\partial x} + (N_1 M_0 + M_1 N_0) S_0^x + M_1 M_0 S_2^x + N_1 N_0 S_3^y, \tag{4.17j}$$

$$A_2 = M_2\frac{\partial A_1}{\partial x} + N_2\frac{\partial A_1}{\partial y} + M_2 B_1 S_1^x + N_2 C_1 S_1^y, \tag{4.17k}$$

$$B_2 = M_2\frac{\partial B_1}{\partial x} + N_2\frac{\partial B_1}{\partial y} + (N_2 B_1 + M_2 C_1) S_0^x + M_2 B_1 S_2^x + N_2 C_1 S_3^y, \tag{4.17l}$$

$$C_{ij} = C_i - C_j. \tag{4.17m}$$

For the further calculation one has to use:

$$\frac{\partial M_n}{\partial x} = \frac{\beta+n}{\beta'+n}\frac{N_n}{x-y}, \qquad \frac{\partial M_n}{\partial y} = \frac{M_n}{x-y}. \tag{4.18}$$

5. The Treatment of the Nuclear Interaction

At energies which are in the neighbourhood or above the Coulomb barrier we have to take into account the influence of the nuclear distortion. In the entrace and exit channel we choose the wavefunctions

$$\begin{aligned} {}^{(N)}\chi_l(r) &= A_l u_l(r) && \text{for } r < R, \\ {}^{(C)}\chi_l(r) &= e^{i\delta_l}(\cos\delta_l F_l(k r) + \sin\delta_l G_l(k r)) && \text{for } r > R, \end{aligned} \tag{5.1}$$

where $G_l(r)$ denotes the irregular Coulomb function and the $u_l(r)$ are eigenfunctions of an optical potential. Both, a square well as well as a Wood-Saxon potential were considered. These potentials determine the phase shifts δ_l. In the case of a complex square well A_l and δ_l are given by:

$$A_l = e^{i\delta_l}\frac{\cos\delta_l F_l(k r) + \sin\delta_l G_l(k r)}{R j_l(\tilde{k} R)} \tag{5.2a}$$

and

$$\delta_l = -\arctan \frac{(l\, j_l(\tilde{k}\, R) - \tilde{k}\, R\, j_{l-1}(\tilde{k}\, R))\, F_l(k\, R) + k\, R\, j_l(\tilde{k}\, R)\, F_l'(k\, R)}{(l\, j_l(\tilde{k}\, R) - \tilde{k}\, R\, j_{l-1}(\tilde{k}\, R))\, G_l(k\, R) + k\, R\, j_l(\tilde{k}\, R)\, G_l'(k\, R)}, \tag{5.2b}$$

where the $j_l(\tilde{k}\, r)$ are Bessel functions with

$$\tilde{k} = \sqrt{k^2 + \frac{2\, m^*}{\hbar^2}\, (V + i\, W)}. \tag{5.3}$$

In the case of a Wood-Saxon potential one can calculate the first few partial waves by numerical integration while the higher partial waves can be obtained with the formulas for pure Coulomb distortion.

6. Coulomb Stripping

One of the most important one-nucleon transfer reaction is the deuteron stripping reaction. The basic formulas for this process can be derived as a special case of equation (3.12). We assume that the deuteron is in a pure s-state and that the proton-neutron interaction can be described by a Hulthén interaction of the form

$$V_{np} \equiv V_{nc} = -V_0 \frac{e^{-\mu r}}{1 - e^{-\mu r}}, \tag{6.1a}$$

with

$$V_0 = \frac{\hbar^2}{M}\, \mu\, (\mu + 2\, \alpha) \qquad \text{and} \quad \alpha = \sqrt{\frac{M\, |\varepsilon_d|}{\hbar^2}} = 0.2317\ F^{-1}. \tag{6.1b}$$

μ^{-1} is the range of the nuclear force. Goldfarb [28] has shown that the d-state of the deuteron can be simulated if one chooses $\mu = 5{,}39\, \alpha$.

The wavefunction corresponding to (6.1) is given by:

$$f_0 = \sqrt{\frac{2\, \alpha\, (\alpha + \mu)\, (2\, \alpha + \mu)}{\mu^2}}\, \frac{e^{-\alpha r}}{r}\, (1 + e^{-\mu r}). \tag{6.2}$$

Substituting (6.1) and (6.2) in (3.12), using $l_1 = 0$ and writing (l_n, m_n) for (l_2, m_2), we get

$$\begin{aligned}\frac{d\sigma}{d\Omega} = \frac{1}{2}\, \bar{\chi}^2 \sum_{m_n} \Bigg| & \sum_{l_i, l_f} i^{l_i - l_f}\, \hat{l}_f\, \hat{l}_i^2\, e^{i(\sigma_{l_i}(\eta_i) + \sigma_{l_f}(\eta_f))}\, Y_{l_f, m_n}(\vartheta, 0) \begin{pmatrix} l_i & l_f & l_n \\ 0 & 0 & 0 \end{pmatrix} \begin{pmatrix} l_i & l_f & l_n \\ 0 & m_n & -m_n \end{pmatrix} \\ & \times \frac{1}{k_i\, \bar{k}_f} \Bigg\{ \int_0^R dr\, {}^{(N)}\chi_{l_i}(r)\, {}^{(N)}\chi_{l_f}\left(\frac{A}{A+1}\, r\right) r^{l_n} \left(\frac{e^{-\varkappa r}}{\varkappa\, r} \sum_{s=0}^{2 l_n} a_s^{l_n}\, r^{-s} \right. \\ & \left. + {}^{(N)}K_{l_n}(\varkappa, \mu, \alpha) \right) + \int_R^\infty dr\, {}^{(C)}\chi_{l_i}(r)\, {}^{(C)}\chi_{l_f}\left(\frac{A}{A+1}\, r\right) \\ & \times \left(h_{l_n}^{(1)}(i\, \varkappa\, r) - {}^{(C)}K_{l_n}(\varkappa, \mu, \alpha) \right) \Bigg\} \Bigg|^2, \end{aligned} \tag{6.3a}$$

with

$$a_s^{l_n} = \sum_{k=0}^{s} c_{s-k}^{k} \left(\frac{-2i\varkappa}{(\alpha+\mu)^2 - \varkappa^2} \right)^k \frac{l_n!}{(l_n-k)!}, \quad c_n^m = \frac{(n+m)!}{n!\,(m-n)!\,(2\varkappa)^n}. \tag{6.3b}$$

The correction terms ${}^{(N)}K_{l_n}(\varkappa, \mu, \alpha)$ and ${}^{(C)}K_{l_n}(\varkappa, \mu, \alpha)$ which are due to penetration effects are relatively small compared to the leading term. This can be seen if one looks at the explicit expression:

$${}^{(N)}K_{l_n}(\varkappa, \mu, \alpha) = \frac{e^{-(\alpha+\mu)r}}{\varkappa r} \sum_{s=0}^{l_n} b_s^{l_n} r^{-s} \tag{6.4a}$$

with

$$b_s^{l_n} = \sum_{k=0}^{l_n} (-)^k \frac{l_n!}{k!\,(l_n-k)!} \sum_{n=0}^{s} \sum_{m=0}^{s-n} c_n^k\, c_m^k \frac{(k-m)!}{(k+n+s)!}$$

$$\times \left(\frac{\alpha+\mu}{(\alpha+\mu)^2-\varkappa^2} \right)^{s-m-n} \left(\left(1 + \frac{\varkappa}{\alpha+\mu} \right)^{s-m-n} - \left(1 - \frac{\varkappa}{\alpha+\mu} \right)^{s-m-n} \right), \tag{6.4b}$$

and

$${}^{(C)}K_{l_n}(\varkappa, \mu, \alpha) = \frac{e^{-(\alpha+\mu)r}}{\varkappa r} \sum_{s=0}^{l_n} \theta_s(\varkappa, \mu, \alpha)\, c_s^{l_n} r^{-s} \tag{6.4c}$$

with

$$\theta_s(\varkappa, \mu, \alpha) = \frac{(-)^{l_n}}{2} \left\{ \frac{\alpha+\mu}{\varkappa} \left(1 - (-)^{s+l_n} \right) + \left(1 + (-)^{s+l_n} \right) \right\}. \tag{6.4d}$$

The parameter $\bar{\chi}^2$ in (6.3a) is given by

$$\bar{\chi}^2 = 16\pi \frac{a\,(a-1)\,A\,(A+1)}{(a+A)^2} \frac{k_f}{k_i} \frac{\hat{J}_f^2}{\hat{J}_i^2} \left(\theta_{j_n, l_n} B(\varkappa)\, N_{l_n} \right)^2, \tag{6.5}$$

where the formfactor $B(\varkappa)$ due to the finite-range neutron-proton interaction is

$$B(\varkappa) = (2\alpha+\mu) \frac{\sqrt{2\alpha\,(\alpha+\mu)\,(2\alpha+\mu)}}{(\alpha+\mu)^2 - \varkappa^2}. \tag{6.6}$$

If the energy of the incident deuteron is well below the Coulomb barrier we can write:

$$\frac{d\sigma}{d\Omega} = \frac{1}{2} \bar{\chi}^2\, G_{l_n}(\vartheta, \eta_i, \eta_f, \varkappa) = \frac{1}{2} \bar{\chi}^2 \sum_{m_n} |F_{l_n, m_n}(\vartheta, \eta_i, \eta_f, \varkappa)|^2, \tag{6.7}$$

where we have used the definitions (3.14c) and (3.14d).

7. The Semiquantal- and Semiclassical Approximations

If we restrict ourselves to energies well below the Coulomb barrier we are allowed to replace the radial wavefunctions describing the scattering process by their WKB-approximation. If we do this, we get for (4.1), using the results of [20],

$$T_{l_i, l_f}^{\lambda, \varkappa} \simeq \frac{1}{4\, k_i\, \bar{k}_f} \frac{\eta}{k} \int_{-\infty}^{+\infty} e^{i(\xi' \varepsilon \sinh w + \xi w)}\, h_\lambda^{(1)} \left(i\varrho\,(1 + \varepsilon \cosh\omega) \right)$$

$$\times \frac{(\cosh w + \varepsilon + i\sqrt{\varepsilon^2 - 1}\sinh w)^\mu}{(\varepsilon \cosh w + 1)^{\mu-1}}\, d\omega = \frac{1}{2\, k_i\, \bar{k}_f\, \varkappa}\, I_{\lambda, \mu}(\varepsilon, \xi, \delta\xi, \varrho), \tag{7.1}$$

with

$$I_{\lambda,\mu}(\varepsilon, \xi, \delta\xi, \varrho) = \int_0^\infty h_\lambda^{(1)}(i\,\varrho\,(1+\varepsilon\cosh\omega))\,\varrho\,(1+\varepsilon\cosh\omega)$$

$$\times\cos\left(\xi'\,\varepsilon\sinh\omega + \xi\,\omega + \mu\arctan\frac{\sqrt{\varepsilon^2-1}\sinh w}{\varepsilon+\cosh w}\right)d\omega\,. \tag{7.2}$$

Hereby we have introduced the dimensionless parameter ϱ which is defined by

$$\varrho = \varkappa\, a_c \equiv \varkappa\,\frac{\eta}{k}\,, \tag{7.3}$$

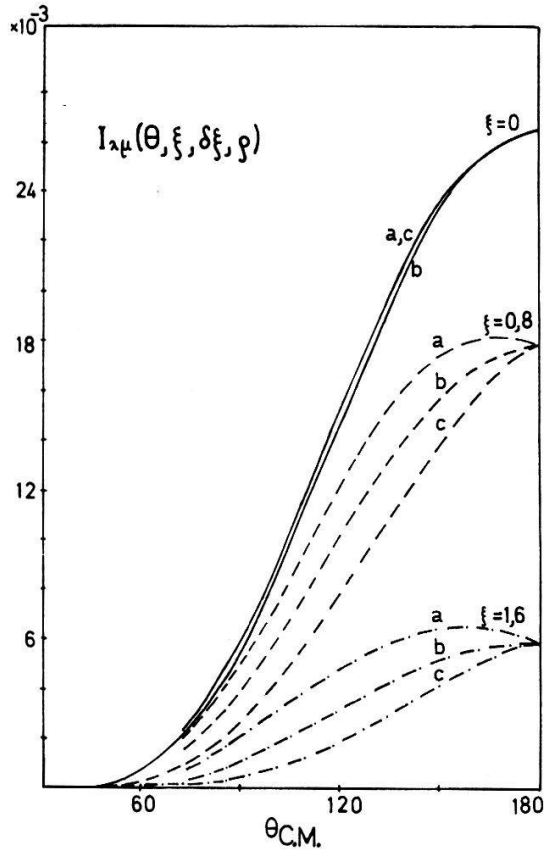

Figure 2
The radial integrals $I_{\lambda,\mu}(\vartheta, \xi, \delta\xi, \varrho)$ with $\lambda = 2$ as a function of ϑ. The ξ-values used for the integrals are indicated in the figure. The curves labelled by a, b and c were calculated with $\mu = -2, 0, +2$ respectively. The ϱ-value used for the curves is $\varrho = 3$. $\delta\xi = 0$.

where a_c is half the distance of closest approach in a head-on-collision.

Furthermore we have

$$\xi' = \xi + \delta\xi = (k_i - \bar{k}_f)\,a_c \tag{7.4a}$$

with

$$\delta\xi = \frac{n}{a-n}\,\frac{\eta_f\,\bar{k}_f}{k}\,, \tag{7.4b}$$

where n is the mass of the transferred particle.

$$\mu = l_f - l_i \quad \text{and} \quad \varepsilon = \frac{1}{\eta}\sqrt{\eta^2 + l\,(l+1)}\,. \tag{7.5}$$

Finally η, k and l are suitable averages of (η_i, η_f), (k_i, k_f) and (l_i, l_f), respectively. For the calculations presented in this paper arithmetic averages were used throughout.

In the case of (d, p)-reactions where $\xi' \simeq -\xi$ equation (7.1) is almost equal to the approximation given by Lemmer [29]. While this approximation agrees quite well with the exact calculation for backward scattering angles, the approximation (7.1) is the better one at small scattering angles.

Substituting (7.1) in (3.14) we get the so called semiquantal approximation.

A further simplification can be obtained by the so called semiclassical treatment, a method well known from the theory of Coulomb excitation [13].

In the semiclassical approximation equation (3.14d) goes over into

$$F_{\lambda,\mu}(\vartheta, \eta_i, \eta_f, \varkappa) \simeq (-)^{\mu} \frac{\eta}{2k^2 \varkappa \sin^2\vartheta/2} \exp\left\{i\left(2\eta\left(\log\left(\frac{\eta}{\sin\vartheta/2}\right) - 1\right) + \frac{\pi}{2}\right)\right\} \sum_m Y_{\lambda,-m}\left(\frac{\pi}{2}, 0\right) D^{\lambda}_{-\mu,-m}\left(\frac{\pi}{2}, \frac{\pi}{2}, \frac{\pi+\vartheta}{2}\right) I_{\lambda,m}(\vartheta, \xi, \delta\xi, \varrho)\,, \tag{7.6}$$

as will be shown in the appendix.

The integral $I_{\lambda,\mu}(\vartheta, \xi, \delta\xi, \varrho)$ in (7.6) is given by (7.2) but now the quantity ε is defined by

$$\varepsilon = \sin^{-1}\frac{\vartheta}{2}\,. \tag{7.7}$$

With this definition it is clear that $I_{\lambda,\mu}(\vartheta, \xi, \delta\xi, \varrho)$ depends now on the scattering angle.

Using the unitarity-relations for the D-functions we get for the differential cross-section:

$$\frac{d\sigma}{d\Omega} = \left(\frac{d\sigma}{d\Omega}\right)_R P(\vartheta)\,, \tag{7.8}$$

where

$$\left(\frac{d\sigma}{d\Omega}\right)_R = \frac{1}{4} a^2 \sin^{-4}\frac{\vartheta}{2} \tag{7.9a}$$

is the Rutherford cross-section and

$$P(\vartheta) = \chi^2 \sum_{\lambda} \begin{pmatrix} j_1 & j_2 & \lambda \\ \frac{1}{2} & -\frac{1}{2} & 0 \end{pmatrix}^2 B_{\lambda}(\vartheta, \xi, \delta\xi, \varrho) \tag{7.9b}$$

gives the probability that a transfer reaction will occur, and where we made furthermore use of the definitions:

$$\chi^2 = \frac{a\,(a-1)\,A\,(A+1)}{(a+A)^2} \frac{k_f}{k_i} \frac{\hat{f}_f^2}{\hat{f}_i^2} \left(\frac{M}{\hbar^2} A^{l_1}_{l_1,0}(\varkappa) \frac{2f(\varrho)}{k\varkappa} \theta_{j_1 l_1} \theta_{j_2 l_2} N_{l_2}\right)^2 \tag{7.10a}$$

with

$$f(\varrho) = e^{-\varrho} K_0(\varrho) \tag{7.10b}$$

and

$$B_{\lambda}(\vartheta, \xi, \delta\xi, \varrho) = \frac{4\pi}{(f(\varrho))^2} \sum_{\mu} |Y_{\lambda,-\mu}\left(\frac{\pi}{2}, 0\right) I_{\lambda,\mu}(\vartheta, \xi, \delta\xi, \varrho)|^2\,. \tag{7.11}$$

We have normalized the function $B_\lambda(\vartheta, \xi, \delta\xi, \varrho)$ such that

$$B_0(\pi, 0, 0, \varrho) = 1 . \tag{7.12}$$

Thus the quantity χ^2 is a measure for the strength of the reaction while its angular dependence is determined by the function $B_\lambda(\vartheta, \xi, \delta\xi, \varrho)$.

In Figure 2 we have represented the integral $I_{\lambda,\mu}(\vartheta, \xi, \delta\xi, \varrho)$ for $\lambda = 2$ and $\mu = -2, 0, +2$ as a function of ϑ, ξ and ϱ with $\delta\xi = 0$.

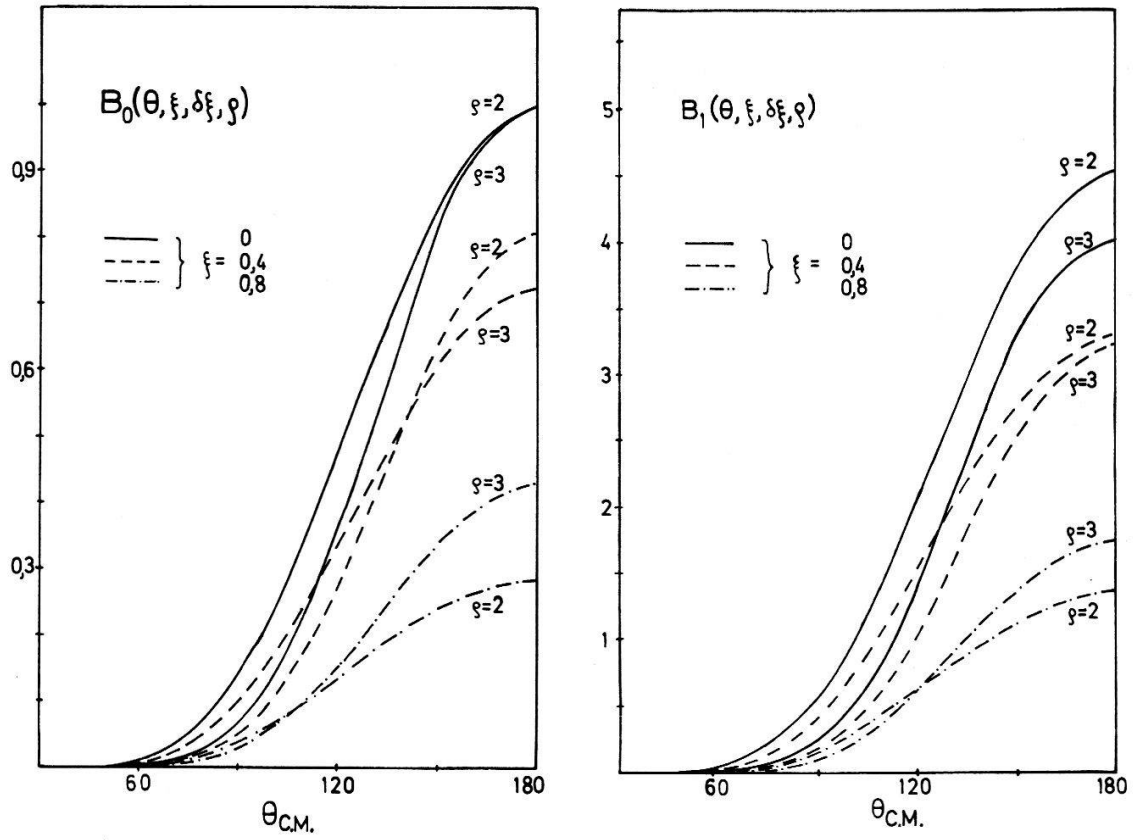

Figure 3
The function $B_\lambda(\vartheta, \xi, \delta\xi, \varrho)$ with $\lambda = 0$ as a function of ϑ. The different curves correspond to the ϱ-values 2, 3 and to the ξ-values 0, 0.4 and 0.8. $\delta\xi = 0$.

Figure 4
Same as in Figure 3, but with $\lambda = 1$.

The integrals are strongly backward peaked and their absolute value decreases rapidly as ξ increases. Figures 3–5 show the function $B_\lambda(\vartheta, \xi, \delta\xi, \varrho)$ for $\lambda = 0, 1, 2$ and for different values of ϱ and ξ as a function of ϑ with $\delta\xi = 0$. These functions have the same qualitative behaviour as the integrals in Figure 2. Since the values of ϱ and ξ are quite similar for different reactions, the functions $B_\lambda(\vartheta, \xi, \delta\xi, \varrho)$ given in Figures 3–5, can be extrapolated for a large variety of reactions.

At this point it is interesting to consider the accuracy of the semiclassical approximation. Comparing the parameters defined by equations (3.14b) and (3.14c) with those defined by (7.10a) and (7.11) we find:

$$\bar{\chi} = \frac{\sqrt{4\pi}\, k\, \varkappa}{f(\varrho)}\, \chi \tag{7.13a}$$

and

$$G_\lambda(\vartheta, \eta_i, \eta_f, \varkappa) \simeq \left(\frac{d\sigma}{d\Omega}\right)_R \left(\frac{f(\varrho)}{k\varkappa}\right)^2 \frac{B_\lambda(\vartheta, \xi, \delta\xi, \varrho)}{4\pi}. \tag{7.13b}$$

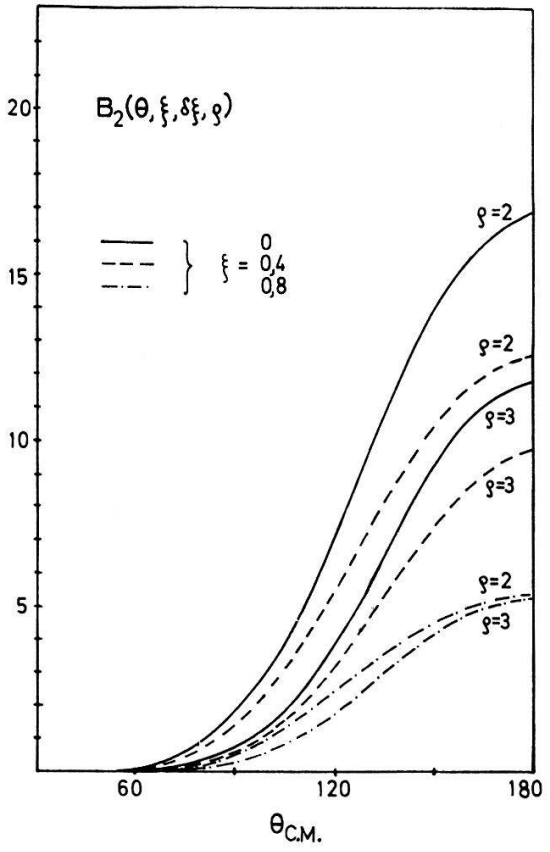

Figure 5
Same as in Figure 3, but with $\lambda = 2$.

We may now define a relative error between the exact calculation and the semi-classical approximation by

$$E_\lambda(\vartheta, \eta, \xi, \delta\xi, \varrho) = \frac{G_\lambda(\vartheta, \eta_i, \eta_f, \varkappa) - G_\lambda^{sc}(\vartheta, \xi, \delta\xi, \varrho)}{G_\lambda(\vartheta, \eta_i, \eta_f, \varkappa)}, \tag{7.14}$$

where $G_\lambda^{sc}(\vartheta, \xi, \delta\xi, \varrho)$ stands for the r.h.s. of equation (7.13b).

In Figure 6 we have represented this function $E_\lambda(\vartheta, \eta, \xi, \delta\xi, \varrho)$ for different values of ϱ and ϑ as a function of $1/\eta^2$. It is evident that the relative error goes with $1/\eta^2$ to zero if η goes to infinity. Hereby we have chosen $\lambda = 1$ and $\xi = \xi' = 0.5$. A further calculation shows that λ as well as ξ and $\delta\xi$ have only a small influence on the error function.

In general we may write

$$E_\lambda(\vartheta, \eta, \xi, \delta\xi, \varrho) = \sum_n c_n(\vartheta, \xi, \delta\xi, \varrho)\, \eta^{-n} \tag{7.15}$$

where the coefficients $c_n(\vartheta, \xi, \delta\xi, \varrho)$ can be extrapolated from Figure 6. Therefore we have approximately:

$$\left(\frac{d\sigma}{d\Omega}\right)_{sc} \simeq \left(\frac{d\sigma}{d\Omega}\right)_{ex} \left(1 - \frac{c_2(\vartheta, \xi, \delta\xi, \varrho)}{\eta^2}\right). \tag{7.16}$$

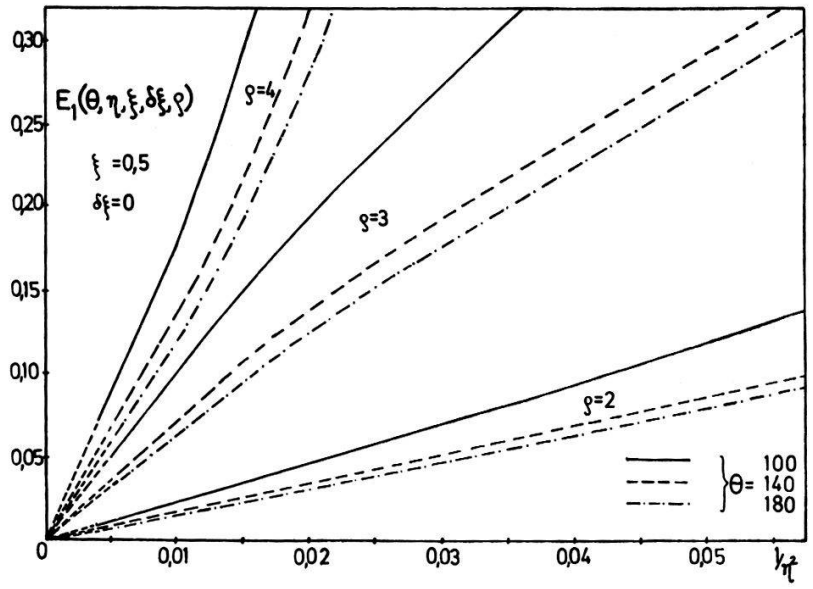

Figure 6
The relative error $E_\lambda(\vartheta, \eta, \xi, \delta\xi, \varrho)$ between the exact calculation and the semiclassical approximation is shown as a function of $1/\eta^2$. The curves were computed with $\lambda = 1$ and different values of ϑ and ϱ as indicated in the figure. The dashed curves for $1/\eta^2 < 0.004$ are extrapolations of the computed curves. The ξ- and ξ'-value used is $\xi = \xi' = 0.5$.

8. Total Cross Sections

In order to investigate the energy dependence of the theory it is interesting to calculate the total cross-section. With the definition

$$\sigma_{tot} = \int \frac{d\sigma}{d\Omega}\, d\Omega \tag{8.1}$$

we get with (3.12)

$$\begin{aligned}\sigma_{tot} = 16\,\pi\, \frac{a\,(a-1)\,A\,(A+1)}{(a+A)^2}\, \frac{k_f}{k_i}\, \frac{\hat{J}_f^2}{\hat{J}_i^2} \left(\frac{M}{\hbar^2}\, \theta_{j_1 l_2}\, \theta_{j_2 l_2}\, N_{l_2}\right)^2 \\ \times \sum_\lambda \begin{pmatrix} j_1 & j_2 & \lambda \\ \frac{1}{2} & -\frac{1}{2} & 0 \end{pmatrix}^2 \hat{\lambda}^2 \sum_{\mu, l_f} \left| \sum_{l_i} i^{l_i - l_f}\, \hat{l}_i^2\, \hat{l}_f\, e^{i(\sigma_{l_i}(\eta_i) + \sigma_{l_f}(\eta_f))} \right. \\ \left. \times \begin{pmatrix} l_i & l_f & \lambda \\ 0 & 0 & 0 \end{pmatrix} \begin{pmatrix} l_i & l_f & \lambda \\ 0 & \mu & -\mu \end{pmatrix} Q_{l_i, l_f}^{l_1, l_2}(j_1, j_2, \lambda, \varkappa) \right|^2 .\end{aligned} \tag{8.2}$$

In the case of pure Coulomb distortion we have to use the radial integrals given by (3.14e) and in the semiquantal approximation by (7.1).

In the semiclassical approximation we get with (7.6)–(7.11):

$$\sigma_{tot} = a_c^2\, \chi^2 \sum_\lambda \begin{pmatrix} j_1 & j_2 & \lambda \\ \frac{1}{2} & -\frac{1}{2} & 0 \end{pmatrix}^2 H_\lambda(\xi, \delta\xi, \varrho) \tag{8.3}$$

with

$$H_\lambda(\xi, \delta\xi, \varrho) = \pi \int_0^\pi \frac{\cos(\vartheta/2)}{\sin^3(\vartheta/2)}\, B_\lambda(\vartheta, \xi, \delta\xi, \varrho)\, d\vartheta\,. \tag{8.4}$$

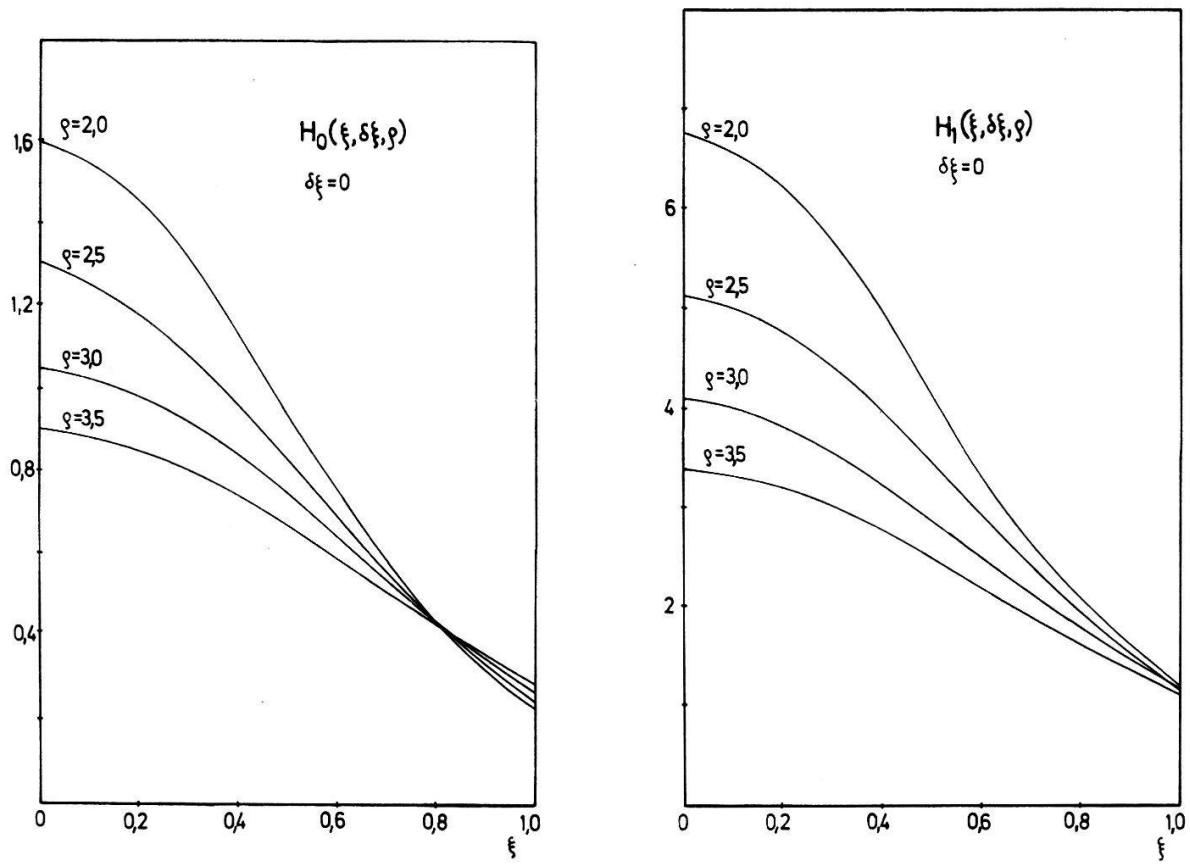

Figure 7
The function $H_\lambda(\xi, \delta\xi, \varrho)$ is shown for $\lambda = 0$ as a function of ξ. The different ϱ-values used are indicated in the figure and $\delta\xi = 0$.

Figure 8
Same as in Figure 7, but with $\lambda = 1$.

Some of these functions $H_\lambda(\xi, \delta\xi, \varrho)$ are given in Figure 7–9 for different values of λ, ξ and ϱ with $\delta\xi = 0$.

In the case of $\lambda = 0$ we can calculate the H_λ-function explicitly. Following [23, 29] we write:

$$I_{0,0}(\vartheta, \xi, \delta\xi, \varrho) = \exp\left(-\varrho - \xi \arctan\frac{\xi'}{\varrho}\right) K_{i\xi}\left(\varepsilon \sqrt{\varrho^2 + \xi'^2}\right). \tag{8.5}$$

Using the integral formula of Lommel [30]

$$\int^z C_\mu(k\,z)\,dz = \frac{z^2}{2}\left\{C_\mu^2(k\,z)\left(1 - \frac{\mu^2}{k^2\,z^2}\right) + C_\mu'^2(k\,z)\right\}, \tag{8.6}$$

where C_μ is any kind of a cylinder function, we get

$$H_0(\xi, \delta\xi, \varrho) = \frac{2\pi\, e^{-2\xi \arctan(\xi'/\varrho)}}{K_0^2(\varrho)} \times \left\{\left(1 + \frac{\xi^2}{\varrho^2 + \xi'^2}\right) K_{i\xi}^2\left(\sqrt{\varrho^2 + \xi'^2}\right) + K_{i\xi}'^2\left(\sqrt{\varrho^2 + \xi'^2}\right)\right\}. \tag{8.7}$$

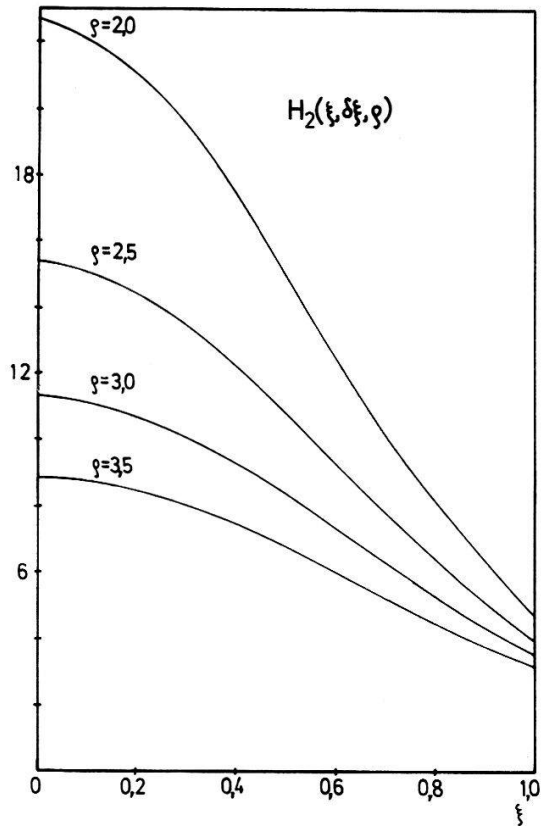

Figure 9
Same as in Figure 7, but with $\lambda = 2$.

9. Polarisation Effects in Deuteron Stripping Reactions

The theory presented in chapter 6 is of course also capable to predict the polarisation of the outgoing proton in a (d, p)-stripping reaction. All measurable quantities in a nuclear reaction can be expressed in terms of the density matrix

$$\varrho_{l\,m,\,l'\,m} = F^{0,0}_{l,m}\, F^{0,0\,*}_{l',m'}, \tag{9.1}$$

where in our case $F^{0,0}_{l,m}$ is given by equation (2.8), or in terms of the statistical tensor

$$\varrho_{k,q}(l, l') = \sum_{m,\,m'} (-)^{l'-m'} \langle l\, m, l' - m' \mid k\, q \rangle\, \varrho_{l\,m,\,l'\,m'}\,. \tag{9.2}$$

The differential cross-section is proportional to $\varrho_{0,0}$, while the vector polarisation is proportional to $\varrho_{1,0}$. Assuming the incident deuterons and the target nuclei to be randomly oriented and assuming that the orientation of the residual nuclei is not measured one finds [31, 32]:

$$P_{l_n}(\vartheta) = \frac{4}{3}\,\frac{(j_n - l_n)}{(2j_n + 1)}\,\frac{\sum_m \sqrt{(l_n + m)\,(l_n - m + 1)}\; Im\,(F^{*}_{l_n,m-1}\, F_{l_n,m})}{\sum_m |F_{l_n,m}\, F^{*}_{l_n,m}|^2}, \tag{9.3}$$

where we have used the definition (3.14d).

Equation (9.3) is only valid for the case of pure Coulomb distortion. At higher energies nuclear spin-orbit interactions must be taken into account.

10. Transfer Reactions in the Diffraction Model

In this chapter we want to discuss the relationship between the results obtained in chapter 3 and 4 and the diffraction model developed by Dar and extended by Frahn and Sharaf and by Suzuki [5–9]. In this model one starts from the general DWBA expression whereby the distorted waves are determined by their asymptotic behaviour. The absorbing effect of the nuclear interaction is taken into account by means of parameters a_l which are given by

$$a_l = \left(1 + i\,\tau\,\frac{\partial}{\partial l}\right) g(l) \tag{10.1a}$$

with

$$g_l = \left(1 + \exp\frac{l_0 - l}{\Delta}\right)^{-1} \tag{10.1b}$$

where l are the orbital momenta of the in and outgoing particle and Δ and τ are arbitrary constants fitted by the experiment.

In the entrance and exit channel l_0 is given by

$$l_0^{i,f} = \frac{x_{i,f}}{|x_{i,f}|}\, k_{i,f}\, R_{i,f} \sqrt{|x_{i,f}|} \quad \text{with} \quad x_{i,f} = 1 - \frac{2\,\eta_{i,f}}{k_{i,f}\, R_{i,f}} \tag{10.2a}$$

and

$$R_i = r_0\,(A^{1/3} + a^{1/3})\,, \quad R_f = r_0\,((A + n)^{1/3} + (a - n)^{1/3})\,, \tag{10.2b}$$

where r_0 is a further arbitrary constant.

Hereby we have modified the original ansatz given by Dar [5] in such a way to include also reactions where $x_{i,f} < 0$.

In the case of a one-nucleon transfer reaction we start with equation (3.14) and get, using (10.1):

$$\frac{d\sigma}{d\Omega} = \bar{\chi}^2 \sum_{\lambda} \begin{pmatrix} j_1\, j_2\, \lambda \\ \frac{1}{2} -\frac{1}{2}\, 0 \end{pmatrix}^2 G_\lambda^{diff}\,(\vartheta, \eta_i, \eta_f, \varkappa) \tag{10.3a}$$

with

$$G_\lambda^{diff}\,(\vartheta, \eta_i, \eta_f, \varkappa) = \hat{\lambda}^2 \sum_{\mu} \Bigg| \sum_{l_i, l_f} i^{l_i - l_f}\, \hat{l}_i^2\, \hat{l}_f\, e^{i(\sigma_{l_i}(\eta_i) + \sigma_{l_f}(\eta_f))}$$

$$\times\, Y_{l_f, \mu}\,(\vartheta, 0) \begin{pmatrix} l_i\, l_f\, \lambda \\ 0\, 0\, 0 \end{pmatrix} \begin{pmatrix} l_i\, l_f & \lambda \\ 0\, \mu & -\mu \end{pmatrix} (a_{l_i}\, a_{l_f})^{1/2}\, T_{l_i, l_f}^{\lambda, \varkappa} \Bigg|^2 . \tag{10.3b}$$

In the case of a multinucleon transfer reaction we have to multiply every function $G_\lambda^{diff}(\vartheta, \eta_i, \eta_f, \varkappa)$ with a structure factor ξ_λ which depends on the special reaction considered. The formulas for these factors for various reactions can be found in [33]. Instead of using approximations of (10.3), based on the localization of $G_\lambda^{diff}(\vartheta, \eta_i, \eta_f, \varkappa)$ in orbital momentum space, we may directly calculate this expression using the results of chapter 4.

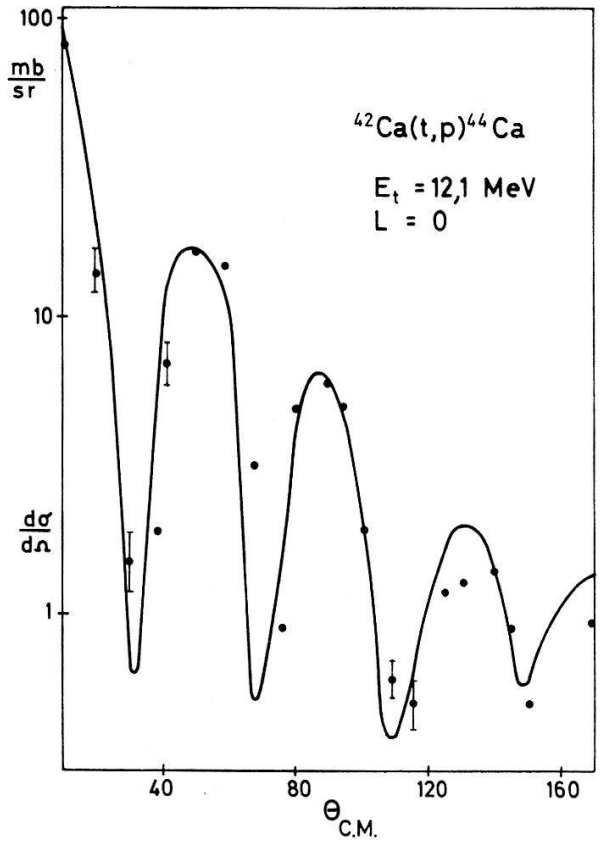

Figure 10
The differential cross-section of the reaction $^{42}Ca(t, p)^{44}Ca$ for a bombarding energy of E_t = 12.1 MeV is shown as a function of ϑ. The curve was calculated with the diffraction model (equation(10.3)) and the experimental values are taken from [34].

In Figure 10 we have represented as a typical example the reaction $^{42}Ca(t, p)^{44}Ca$ [34] at a bombarding energy of 12,1 MeV. While the fit given by $r_0 = 1.05$ fm, $\Delta = 0.25$ and $\tau = 0.8$ is quite similar to the one given by Frahn and Sharaf, the spectroscopic factors extracted from the two models differ by a factor 1.5.

Calculations of other reactions are in preparation.

11. Numerical Results and Discussion

a) *Calculation of the Coulomb integrals*

Here we give a brief survey of the numerical procedure leading to the radial integrals (4.1) necessary for calculating (3.12).

Point of departure are the maximal matrixelements with $\lambda = 0$ and $\lambda = 1$. Starting with equations (4.6) and (4.7) we first calculate $M_{0,0}^{-1,\varkappa}$, $M_{1,1}^{-1,\varkappa}$ and $M_{1,0}^{-2,\varkappa}$, $M_{2,1}^{-2,\varkappa}$, $M_{3,2}^{-2,\varkappa}$ and subsequently by using equations (4.18), (4.21) and (4.11) the other maximal matrixelements with $\lambda = 0,1$. From equation (4.15) we obtain $M_{l+1,l}^{-1,\varkappa}$ and $M_{l,l+1}^{-1,\varkappa}$. Putting in (4.16b) $n = 0$ and $p = 1, 2, 3, \ldots$ we obtain all the matrix-elements $M_{l+p+1,l}^{-1,\varkappa}$ satisfying the triangular condition $|l_i - l_f| \leqslant \lambda \leqslant l_i + l_f$. Next we determine all integrals $M_{l,l}^{-2,\varkappa}$ by using equation (4.16a) with $p = n = 0$, and all matrixelements $M_{l+p+1,l}^{-2,\varkappa}$ by putting in equation (4.16b) $n = 1$ and $p = 1, 2, 3, \ldots$. Together with equation (4.11) we obtain by repeated application of equation (4.16) all those matrixelements which are necessary for the integral $T_{l_i,l_f}^{\lambda,\varkappa}$.

b) *Calculation of the reaction amplitude*

A difficulty arises in the determination of the reaction amplitude (3.14d) because for large values of η a large number of angular momenta contribute to the sum and the

convergence is very bad. The convergence can be improved by means of a method which is frequently used in electron scattering [35] and Coulomb excitation calculations [36]. The reaction amplitude (3.14d) is of the form

$$F_{\lambda,\mu}(\vartheta, \eta_i, \eta_f, \varkappa) = \sum_l c_{l,\mu}\, Y_{l,\mu}(\vartheta, 0)\,. \tag{11.1}$$

It is now useful to define a new coefficient $c^{(1)}_{l,\mu}$ so that we can write for the reaction amplitude:

$$F_{\lambda,\mu}(\vartheta, \eta_i, \eta_f, \varkappa) = \frac{1}{1-\cos\vartheta} \sum_l c^{(1)}_{l,\mu}\, Y_{l,\mu}(\vartheta, 0)\,, \tag{11.2}$$

where the new coefficients $c^{(1)}_{l,\mu}$ are connected with the $c_{l,\mu}$ by a simple recursion formula.

By repeated application of this formula (e.g. k times, with $k \simeq 3$–5) the number of angular momenta necessary for the computation of $F_{\lambda,\mu}(\vartheta, \eta_i, \eta_f, \varkappa)$ can be reduced considerably (in our case by a factor of about 1/3) and the convergence becomes very good. The recursion relation for the coefficients is given by

$$\begin{aligned} c^{(k)}_{l,\mu} = c^{(k-1)}_{l,\mu} &- \left(\frac{(l+\mu)\,(l-\mu)}{(2\,l+1)\,(2\,l-1)}\right)^{1/2} c^{(k-1)}_{l-1,\mu} \\ &- \left(\frac{(l+1+\mu)\,(l+1-\mu)}{(2\,l+3)\,(2\,l+1)}\right)^{1/2} c^{(k-1)}_{l+1,\mu}\,. \end{aligned} \tag{11.3}$$

c) *Comparison with experiments*

α) Heavy ion transfer reactions

As a typical example of a one-nucleon transfer reaction we have chosen the well studied ^{14}N (^{13}N, ^{13}N) ^{15}N-reaction [37] with $(l_1, j_1) = (1, 1/2)$ and $(l_2, j_2) = (1, 1/2)$. In Figure 11 we have compared the exact calculation with pure Coulomb distortion with the two corresponding approximations discussed in chapter 7. The three curves were calculated with equations (3.14), (7.1) and (7.8), respectively. The exact curve is quite similar to the one derived in a somewhat different way by Buttle and Goldfarb [10]. We have taken into account the identity of the two ^{14}N in the entrance channel by the method outlined in [10]. From the exact calculation and the experimental data the spectroscopic factor $(\theta_{j_1 l_1}\, \theta_{j_2 l_2})^2 = 0.217$ was obtained. The semiquantal and semiclassical calculation were performed using the same spectroscopic factor. It is evident from Figure 11 that the semiquantal and to a somewhat lesser degree the semiclassical calculations approximate the exact theory rather well. Figure 12 demonstrates the influence of the nuclear distortion. Combining equations (3.12) and (3.7e) one finds immediately

$$g_1(r) = \frac{e^{-\varkappa r}}{\varkappa r}\left\{A^1_{1,0}(\varkappa)\left(1+\frac{1}{\varkappa r}\right) - \frac{1}{r}\,A^1_{0,1}(\varkappa)\right\} + \frac{1}{r}\,K^1_{0,1}(\varkappa) - K^1_{1,0}(\varkappa)\,. \tag{11.4}$$

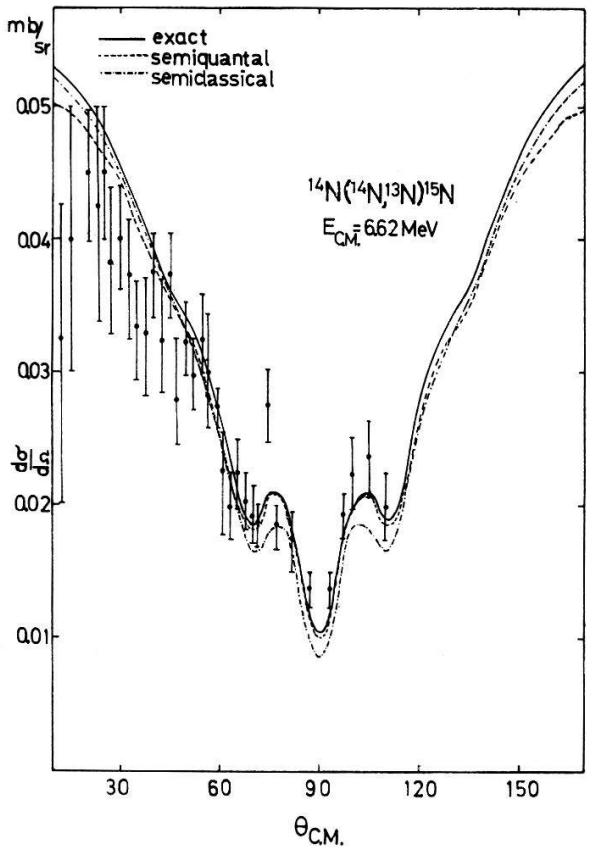

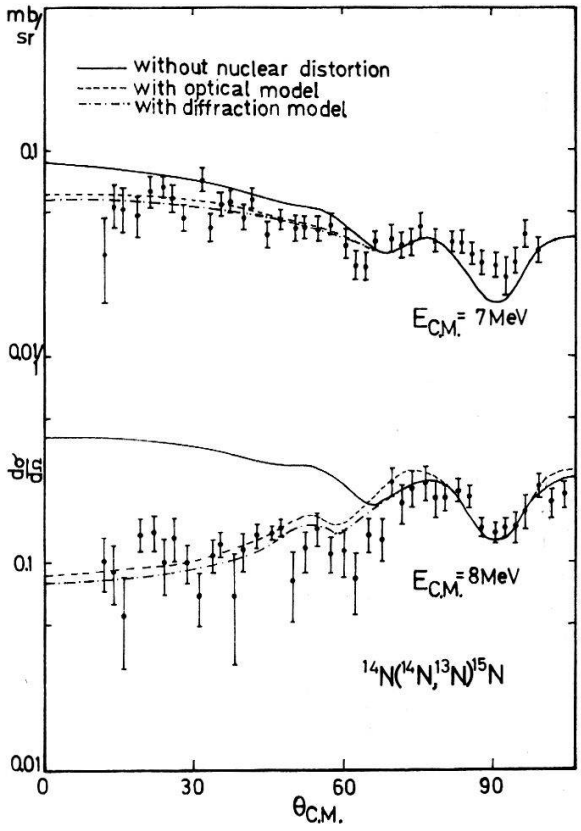

Figure 11
Angular distribution of the reaction $^{14}N(^{14}N, ^{13}N)^{15}N$ at E_{CM} = 6.62 MeV. The exact curve, calculated with equation (3.12) by neglecting the nuclear distortion is compared with the semiquantal and the semiclassical approximation. The experimental values are those of [37].

Figure 12
Angular distribution of the reaction $^{14}N(^{14}N, ^{13}N)^{15}N$ at E_{CM} = 7 MeV and E_{CM} = 8 MeV. The influence of the nuclear distortion is shown. The full line gives the calculation for pure Coulomb distortion, while the dashed curves include the effect due to nuclear distortion. The experimental values are taken from [37].

It is easy to see that for the present case the correction terms $K^1_{0,1}(\varkappa)$ and $K^1_{1,0}(\varkappa)$ can be neglected. With the help of a recursion relation for the spherical Bessel functions and using the fact that $A^1_{1,0}(\varkappa)$ is in a good approximation proportional to $\varkappa$ [10] one obtains

$$g_1(r) \simeq \frac{e^{-\varkappa r}}{\varkappa r} A^1_{1,0}(\varkappa) \left(r + \frac{1+3i}{\varkappa}\right). \tag{11.5}$$

By means of equation (11.5) the lowest 3–5 (depending on energy) partial waves of (3.12) were calculated. The higher partial waves were obtained using the formulas for pure Coulomb distortion. For simplicity the distorting optical potential was chosen to be a complex square well with $V = -50$ MeV, $W = -30$ MeV and $R = 7.2$ fm for both the entrance and the exit channel. Furthermore we have calculated the nuclear distortion with the help of the diffraction model (equation 10.3) with $r_0 = 1.95$, $\Delta = 1.6$ and $\tau = 0$. Figure 13 shows the total cross-section calculated by means of equation (8.2).

β) Deuteron stripping reactions

Figures 14–16 show some examples of deuteron stripping calculations. Figure 14 illustrates the validity of the semiquantal and semiclassical approximation in the case of the ^{209}Bi$(d, p)^{210}$Bi reaction [38].

It can be seen that these approximations are not quite satisfactory. This is due to the fact that the value of $\delta\xi$ is much greater than for heavy ion transfer reactions.

In Figure 15 we have repeated the calculations for the reaction ^{138}Ba$(d, p)^{139}$Ba [39], for different bombarding energies and Q-values. One sees that at low energies all three curves which were calculated with the same spectroscopic factor represent the angular dependence quite well, while their absolute values differ considerable. At higher energies nuclear distortion effects become important. This can be seen from Figure 16 in which the dashed curve represents a calculation for one of the $l_n = 1$ transitions in ^{138}Ba in which a square well with $V_d = -80$ MeV, $W_d = -56$ MeV, $V_p = -48$ MeV, $W_p = -52$ MeV and $R = 7.4$ fm as well as the diffraction model with $r_0 = 1.8$, $\Delta = 1.1$ and $\tau = 0$ was used to simulate nuclear distortion. Thus nuclear distortion has the effect of reducing the differential cross-section at backward angles.

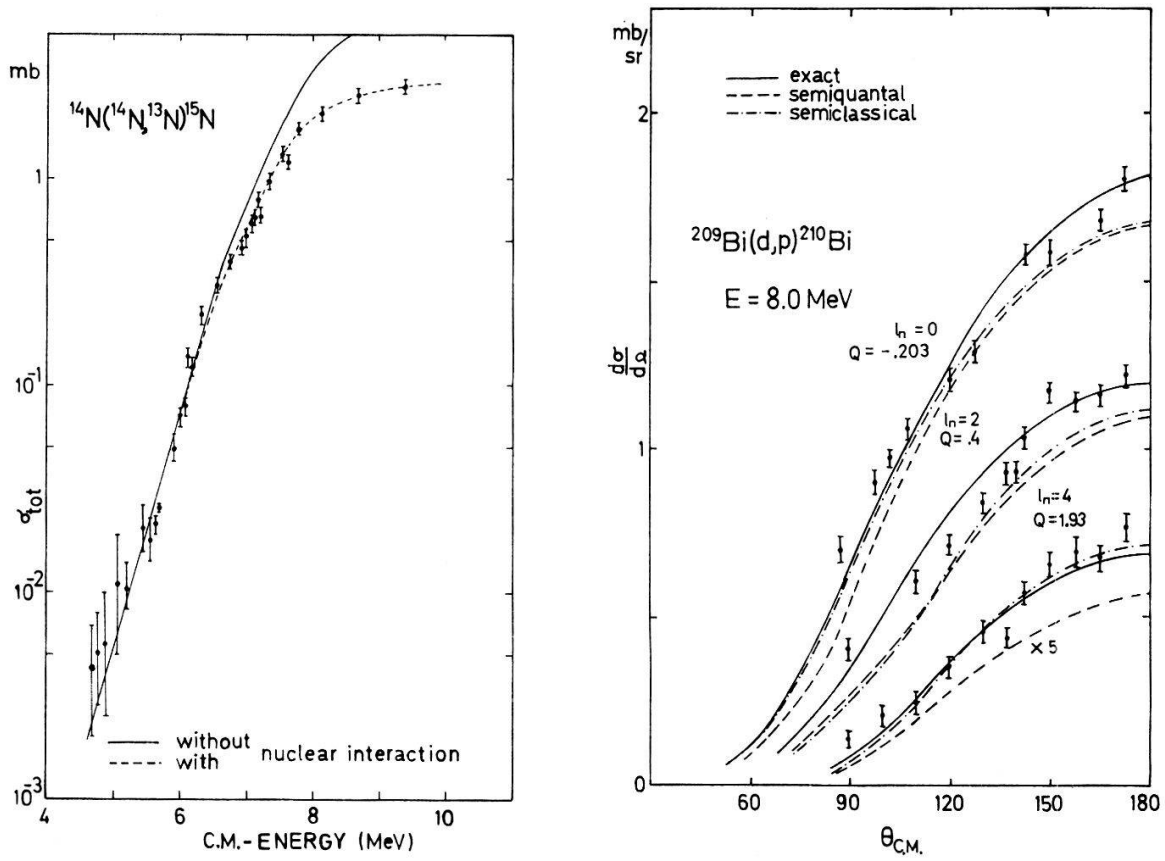

Figure 13
The total cross-section is calculated for the reaction ^{14}N(^{14}N, ^{13}N)^{15}N for pure Coulomb distortion (full line) and including nuclear distortion (dashed curve) as a function of the center of mass energy. The experimental values are taken from [37].

Figure 14
Angular distribution of the reaction ^{209}Bi$(d, p)^{210}$Bi at $E_{CM} = 8.0$ MeV and for l_n-values $l_n = 0, 2, 4$. The exact curve due to equation (3.12) is compared with its semiquantal and semiclassical approximation. The nuclear distortion is neglected. The experimental values are taken from [38].

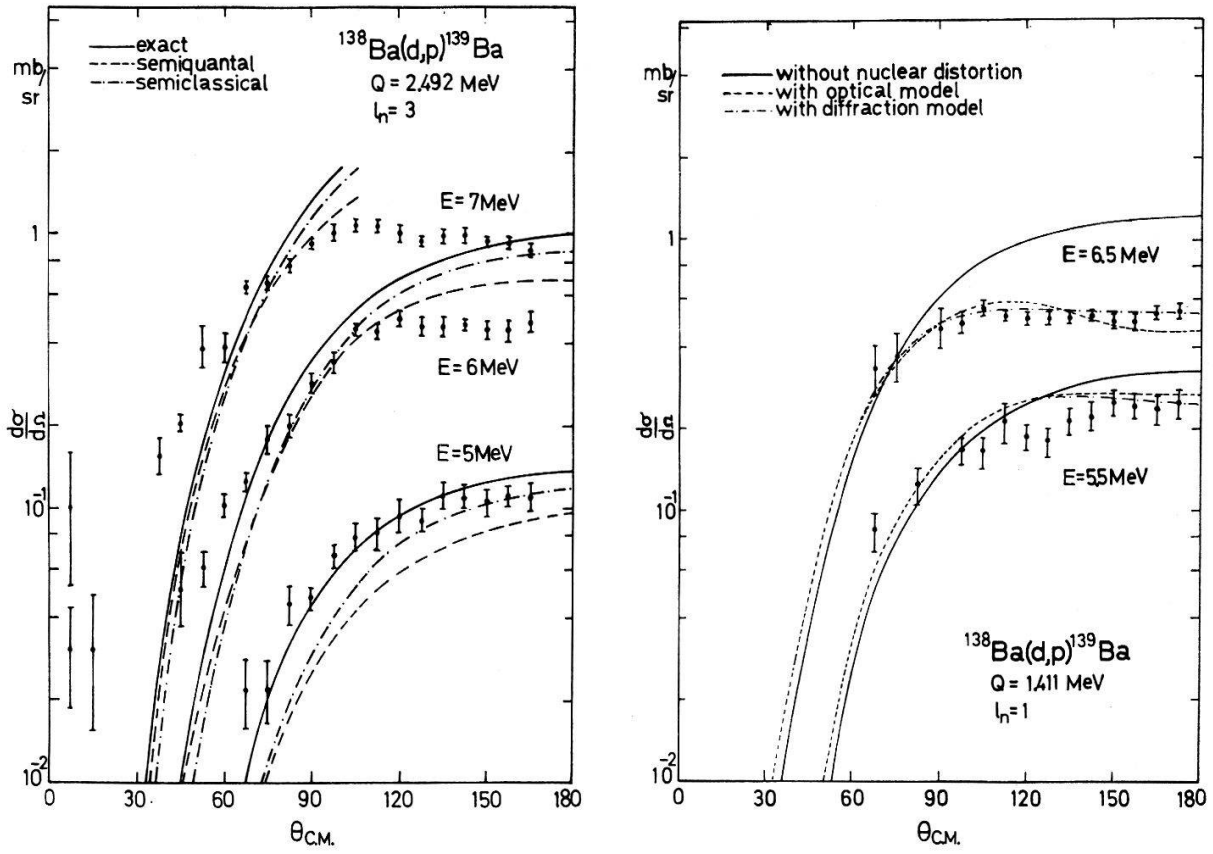

Figure 15
The same as in Figure 14, but for the ^{138}Ba$(d, p)^{139}$Ba reaction at $E_{CM} = 5$, 6 and 7 MeV and with $l_n = 3$. The experimental values are those of [39].

Figure 16
The influence of the nuclear distortion is shown for the ^{138}Ba$(d, p)^{139}$Ba reaction at $E_{CM} = 5.5$ and $E_{CM} = 6.5$ MeV and with $l_n = 1$. The full line corresponds to pure Coulomb distortion, while the dashed lines were computed with nuclear distortion.

It is clear from Figure 16 that inclusion of nuclear distortion improves the agreement with experiment considerably for energies close to the Coulomb barrier.

γ) Polarisation calculations

To our knowledge there exist no polarisation experiments for deuteron stripping reactions below the Coulomb barrier. In Figure 17 we show the predictions of our theory for the ^{209}Bi$(d, p)^{210}$Bi reaction.

The influence of the transferred orbital angular momentum on the polarisation is shown. The similar behaviour of the polarisation curve for different values of l_n at backward angles is remarkable. The ascent of the curves is linear at $\vartheta \simeq \pi$ and proportional to the value of l_n. It thus appears that in this region the polarisation is proportional to the derivative of $d\sigma/d\Omega$. The dependence of the polarisation on the transferred angular momentum j_n (i.e. $j_n = l_n \pm 1/2$) is given by the well known expression

$$P_{l_n+\frac{1}{2}} = -\frac{l_n}{l_n+1} P_{l_n-\frac{1}{2}}. \tag{11.6}$$

Hence if the polarisation below the Coulomb barrier can be measured the value of j_n can be determined in an unambigious and model independent manner.

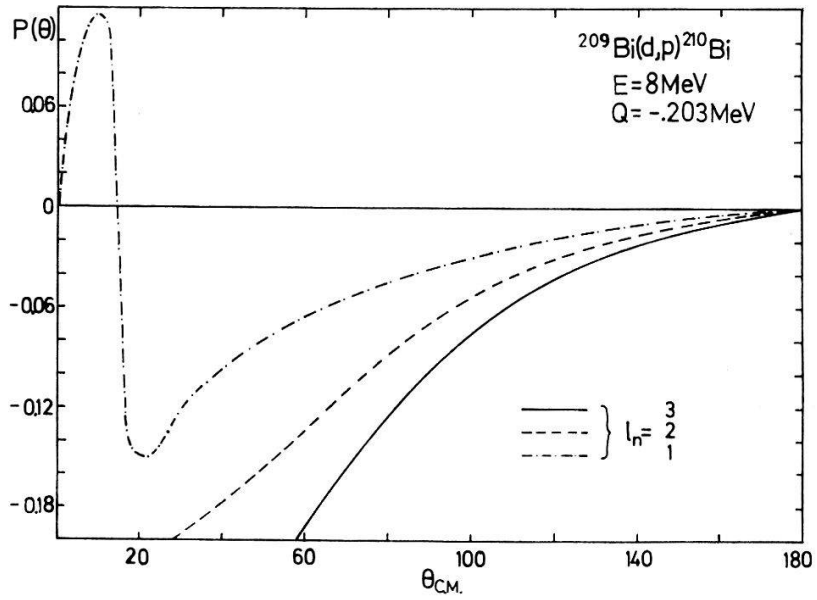

Figure 17
The influence of the orbital angular momentum of the transferred neutron on the polarization is shown. All three curves were calculated by means of equation (9.4) without any nuclear distortion for the ^{209}Bi$(d, p)^{210}$Bi reaction. The center of mass energy was assumed to be 8 MeV and the l_n-values taken were $l_n = 1, 2, 3$.

Acknowledgements

The numerical calculations have been performed on an UNIVAC 1108 at the SANDOZ A.G., Basel. We would like to thank the staff of the 'Rechenzentrum' for their help and advice. We are indepted to dipl. phys. T. Ledergerber and dipl. phys. R. Mülhauser for help in the calculations, and to dipl. phys. R. Morf for some discussions concerning the semiclassical approximation. We thank Prof. L. J. B. Goldfarb for a discussion and for pointing out an error that arose in an earlier version of this work. One of the authors (D.T.) is indepted to the Swiss National Foundation for a grant.

Appendix

Here we give the derivation of the semiclassical formula (7.6). Starting point is equation (3.14d)

$$F_{\lambda,\mu}(\vartheta, \eta_i, \eta_f, \varkappa) = \hat{\lambda} \sum_{l_i, l_f} \hat{l}_f \hat{l}_i^2 \, e^{i(\sigma_{l_i}(\eta_i)+\sigma_{l_f}(\eta_f))} \, i^{l_i - l_f}$$
$$\times \begin{pmatrix} l_i & l_f & \lambda \\ 0 & 0 & 0 \end{pmatrix} \begin{pmatrix} l_i & l_f & \lambda \\ 0 & \mu & -\mu \end{pmatrix} Y_{l_f,\mu}(\vartheta, 0) \, T^{\lambda,\varkappa}_{l_i, l_f}, \tag{A.1}$$

in which we insert the following expressions for the 3-j-symbols, the Coulomb phase shift and the spherical harmonics, applicable if $l_i, l_f \gg \lambda, 1$:

$$\begin{pmatrix} l_i & l_f & \lambda \\ m_i & m_f & \mu \end{pmatrix} \simeq \frac{(-)^{l_i+m_f}}{\hat{l}_i^2} D^{\lambda}_{\mu, l_i - l_f}(0, \beta, 0), \qquad \cos\beta = -\frac{m_i}{l_i}, \tag{A.2}$$

$$Y_{l,m}(\vartheta, 0) \simeq \frac{1}{\pi \sqrt{\sin\vartheta}} \cos\left(\left(l + \frac{1}{2}\right)\vartheta - \frac{\pi}{4} + \frac{m\pi}{2}\right) \tag{A.3}$$

and

$$\sigma_l(\eta) = Im \log\Gamma(l + 1 + i\eta) \simeq \left(l + \frac{1}{2}\right) \arctan\frac{\eta}{l+1} + \frac{\eta}{2}\log((l+1)^2 + \eta^2) - \eta + 0\left(\frac{1}{\eta}\right). \tag{A.4}$$

We have used the definition of Edmonds [40] for the D-functions. We substitute in (A.1) the radial integral by its WKB-approximation (7.1). Using average values for the physical quantities appearing in (A.1) we obtain:

$$F_{\lambda,\mu}(\vartheta, \eta_i, \eta_f, \varkappa) \simeq \frac{1}{\pi}\sum_{l,m} \hat{l}\,\frac{1}{\sqrt{\sin\vartheta}}\, i^{-m} \cos\left(\left(l + \frac{1}{2}\right)\vartheta - \frac{\pi}{4} - \mu\frac{\pi}{2}\right) \times d^{\lambda}_{0,-m}\left(\frac{\pi}{2}\right) d^{\lambda}_{-\mu,-m}\left(\frac{\pi}{2}\right) \exp\left\{i\,(2l + 1 - m)\arctan\frac{\eta}{l+1} + \eta\log((l+1)^2 + \eta^2) - 2\eta\right)\right\} \frac{1}{2k^2\varkappa}\, I_{\lambda,m}(\varepsilon, \xi, \delta\xi, \varrho). \tag{A.5}$$

This expression can be evaluated by the method of steepest descent [41], whereby the sum

$$f = \sum_l A(l)\, e^{iB(l)}. \tag{A.6}$$

is approximated by

$$f \simeq A(l_0)\sqrt{\frac{\pi}{i\beta}}\, e^{iB(l_0)}. \tag{A.7}$$

The quantity β in this last expression is given by

$$\beta = \frac{1}{2}\frac{d^2B(l)}{dl^2}\bigg|_{l=l_0} \tag{A.8}$$

and l_0 is determined by

$$\frac{dB}{dl}\bigg|_{l=l_0} = 0. \tag{A.9}$$

In our case equation (A.9) leads to

$$l_0 + 1 = \eta\,\mathrm{cotan}\,\frac{\vartheta}{2}. \tag{A.10}$$

Using (A.7) and (A.10) we get from equation (A.5) after some trivial calculations the desired result (7.6).

REFERENCES

[1] G. Breit and M. Ebel, Phys. Rev. *103*, 103 (1956); *104*, 1030 (1956).
[2] G. Breit, K. W. Chun and H. G. Washweiler, Phys. Rev. *133*, B404 (1964).
[3] G. Breit, J. A. Polak and D. A. Torchia, Phys. Rev. *161*, 933 (1967).
[4] A. Dar, Phys. Rev. *139*, B1193 (1965); Nucl. Phys. *82*, 354 (1966).
[5] W. Frahn and M. Sharaf, Nucl. Phys. *133*, A133 (1969).
[6] T. Suzuki, Progr. Theor. Phys. *39*, 83 (1968); *41*, 695 (1969).
[7] N. Austern, R. M. Drisko, E. C. Halbert and G. R. Satchler, Phys. Rev. *133*, B3 (1964).
[8] T. Kammuri and H. Yoshida, Nucl. Phys. *129*, A625 (1969).
[9] T. L. Abelishvili, JETP *40*, 1440 (1961).
[10] P. J. A. Buttle and L. J. B. Goldfarb, Nucl. Phys. *78*, 409 (1966).
[11] L. J. B. Goldfarb and E. Parry, Nucl. Phys. *116*, A309 (1968).
[12] L. J. B. Goldfarb and J. W. Steed, Nucl. Phys. *116*, A321 (1968).
[13] K. Alder and A. Winther, *Coulomb Excitation* (Academic Press, New York 1966).
[14] F. B. Morinigo, Phys. Rev. *134*, B1243 (1964).
[15] M. El-Nadi and T. H. Rihan, Proc. Phys. Soc. *87*, 119 (1966).
[16] M. Danos and L. C. Maximom, J. Math. Phys. *6*, 766 (1965).
[17] M. Moshinsky, Nucl. Phys. *13*, 104 (1959).
[18] K. A. Ter-Martirosyan, JETP *2*, 620 (1956).
[19] K. Alder and A. Winther, Kgl. Danske Videnskab. Selskab Mat. Fys. Medd. *29*, Nos. 18 and 19 (1955).
[20] K. Alder, A. Bohr, T. Huus, B. Mottelson and A. Winther, Rev. Mod. Phys. *28*, 432 (1956).
[21] P. Appell and Kampe de Feriet, *Fonctions Hypergéometriques et Hypersphériques* (Gauthier-Villars, Paris 1926).
[22] A. Erdelyi et al., *Higher Transcendental Functions*, Vol. I, p. 222–245 (McGraw-Hill Book Company Inc., New York 1953).
[23] D. Trautmann and K. Alder, Proc. Conf. Nuclear reactions induced by heavy ions, Heidelberg (1969), in print.
[24] K. Alder and D. Trautmann, Proc. Conf. Properties of nuclear states, Montreal (1969), in print.
[25] P. O. M. Olsson, Arkiv Fysik *30*, 187 (1965); *29*, 459 (1965).
[26] H. Almström and P. Olsson, J. Math. Phys. *8*, 2013 (1966).
[27] G. E. Hahne, J. Math. Phys. *10*, 524 (1968).
[28] L. J. B. Goldfarb, Phys. Lett. *24B*, 264 (1967).
[29] R. H. Lemmer, Nucl. Phys. *39*, 680 (1962).
[30] G. N. Watson, *Theory of Bessel Functions*, 2nd ed. (Cambridge University Press, New York 1944), p. 135.
[31] R. Huby, M. Y. Refai and G. R. Satchler, Nucl. Phys. *9*, 94 (1958).
[32] W. Tobocman, *Theory of Direct Nuclear Reactions* (Oxford University Press, Oxford 1961), p. 69.
[33] N. K. Glendenning, Ann. Rev. Nucl. Sci. *13*, 191 (1963).
[34] B. F. Bayman and N. M. Hintz, Phys. Rev. *172*, 1113 (1968).
[35] D. R. Yennie, D. G. Ravenhall and R. N. Wilson, Phys. Rev. *95*, 500 (1954).
[36] K. Alder and H. K. Pauli, Nucl. Phys. *128*, 193 (1969).
[37] J. C. Hiebert, J. A. McIntrye and J. G. Couch, Phys. Rev. *138*, B346 (1965).
[38] J. R. Erskine, W. W. Buechner and H. A. Enge, Phys. Rev. *128*, 720 (1962).
[39] J. Rapaport and A. K. Kerman, Nucl. Phys. *119*, A641 (1968).
[40] A. R. Edmonds, *Angular Momentum in Quantum Mechanics* (Princeton University Press, Princeton 1957).
[41] Mott and Massey, *The Theory of Atomic Collisions*, 2nd ed. (Oxford 1949), p. 12.